pH-controlled DNA- and RNA-templated assembly of short oligomers

Renaud Barbeyron, Jean-Jacques Vasseur and Michael Smietana**

ELECTRONIC SUPPLEMENTARY INFORMATION

Pages

List of Tables and Figures

Pages

General

All reagents were purchased from Aldrich or local suppliers and used without purification. All unmodified oligonucleotides used for this study were purchased from Eurogentec. Synthesized 5' borono-oligonucleotides were purified by RP-HPLC (Dionex Ultimate 3000) with a Nucleodur 100-7 C18 column (125 x 8 mm; Macherey-Nagel) and analyzed with a Nucleodur 100-3 C18 column (75 x 4.6 mm; Macherey-Nagel) and by MALDI-TOF MS (Voyager PerSeptive Biosystems) using trihydroxyacetophenone (THAP) as matrix and ammonium citrate as co-matrix. Thermal denaturation experiments were performed on a VARIAN Cary 300 UV spectrophotometer equipped with a Peltier temperature controller and a thermal analysis software. Native PAGE experiments were performed on a Hoefer SE600X apparatus and revealed by UV-shadowing. CD spectra were recorded using a JASCO J-815 CD Spectrometer, wavelengths were scanned in the 210-340 nm range with a scanning speed of 100 $nm.min^{-1}$.

Syntheses of 5' boronooligonucleotides

Syntheses were performed in 1µmol scale using an ABI 381A DNA synthesizer by phosphoramidite chemistry with conditions described in Table S1. dT^{bn}-phosphoramidite was synthesized and incorporated at the 5'-end of an oligonucleotide according to previous records.[1,2]

Table S1. Coupling conditions for oligonucleotides syntheses.

Step	Reaction	Reagent	Time (s)
1	Deblocking	3% TCA in DCM	35
2	Coupling	0.1M amidite in CH_3CN + 0.3M BMT in CH3CN	20
3	Capping	Ac_2O/THF/Pyridine + 10% NMI in THF	8
4	Oxidation	0.1M I_2 in THF/H_2O/Pyridine	15

[1] D. Luvino, C. Baraguey, M. Smietana, J. J. Vasseur, *Chem. Commun.* **2008,** 2352.
[2] A. R. Martin, I. Barvik, D. Luvino, M. Smietana, J. J. Vasseur, *Angew. Chem.* **2011,** *50,* 4193.

Analyses of 5' boronooligonucleotides

HPLC and MALDI-TOF analysis of 5'-T^{bn}GTGTA-3'

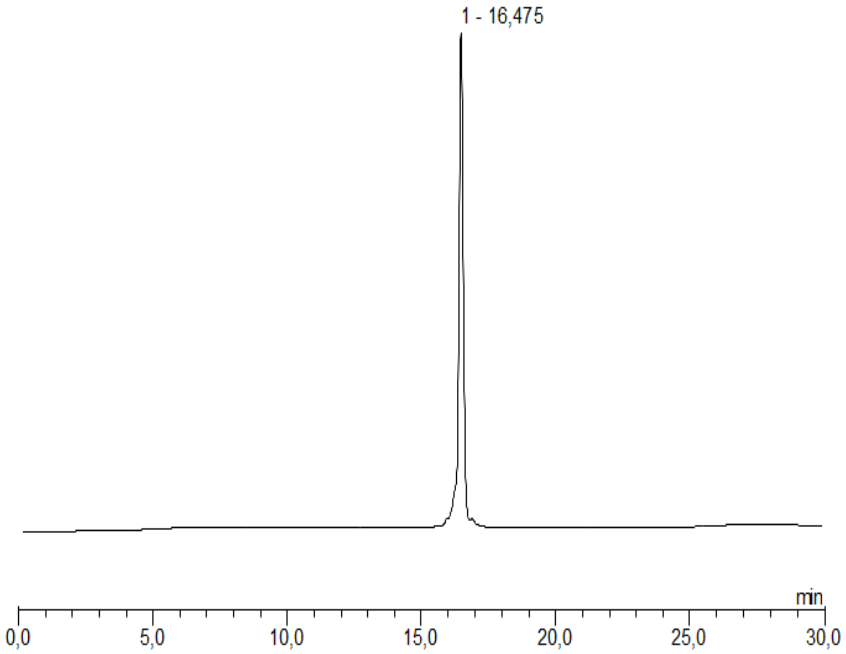

HPLC conditions analysis: Column Nucleodur C18, 100 Å, 3 µm, elution with a linear gradient of 0 to 20% CH_3CN in triethylammonium acetate buffer, pH 7, in 30min, Flow rate 1 mL.min^{-1}, λ 260 nm.

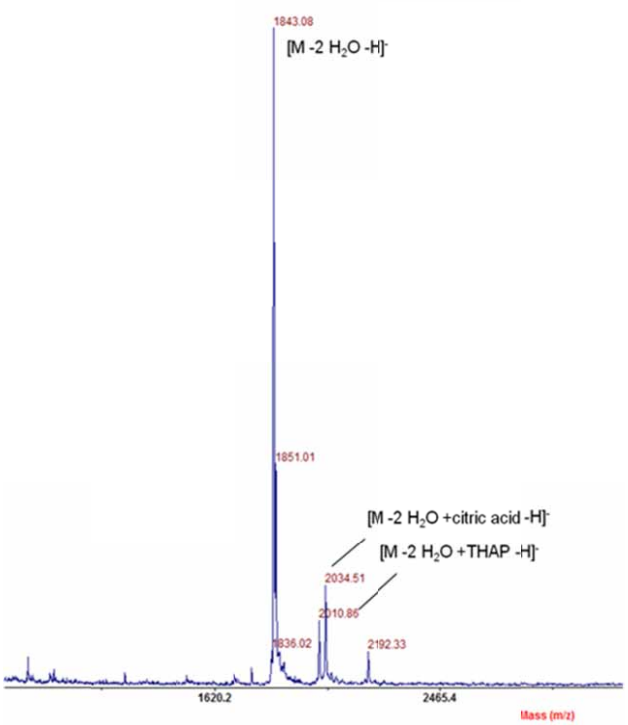

MALDI-TOF MS conditions analysis: ionization in negative mode, THAP (MW= 168.15 g.mol^{-1}) as matrix and ammonium citrate (MW= 243.2 g.mol^{-1}) as co-matrix, delay time 100 ns and an acceleration voltage of 24 kV.

*HPLC and MALDI-TOF analysis of 5'-T^{bn}CATC**A**-3'*

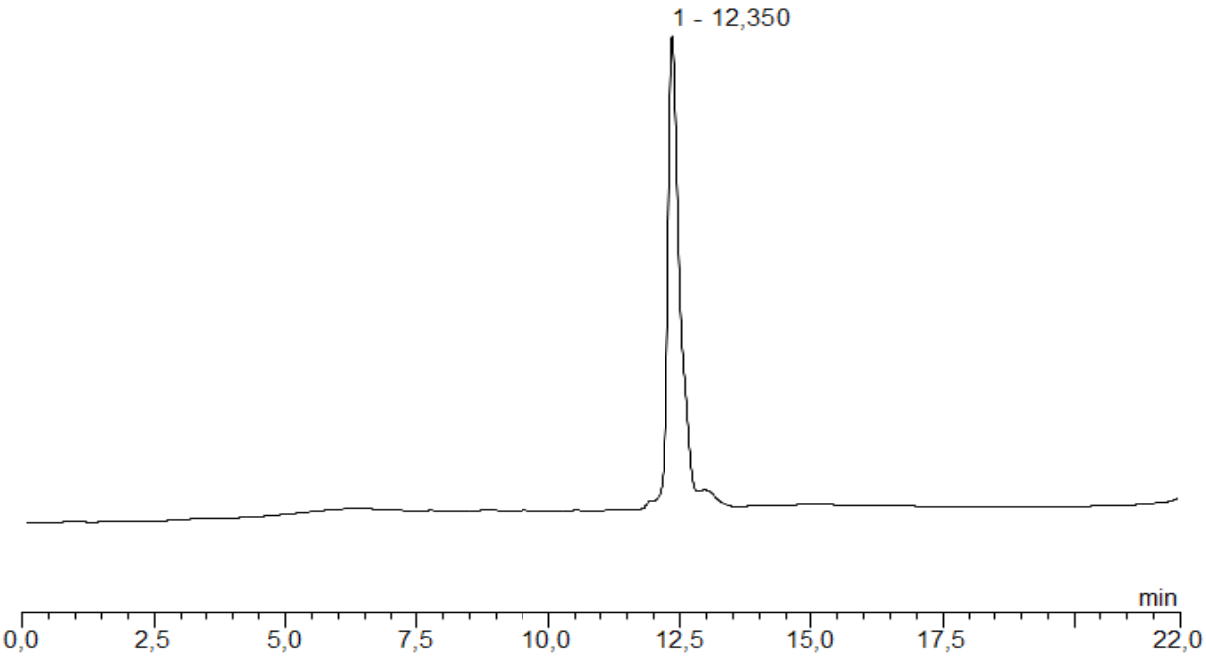

HPLC conditions analysis: Column Nucleodur C18, 100 Å, 3 µm, elution with a linear gradient of 0 to 20% CH_3CN in triethylammonium acetate buffer, pH 7, in 20min, Flow rate 1 mL.min^{-1}, λ 260 nm.

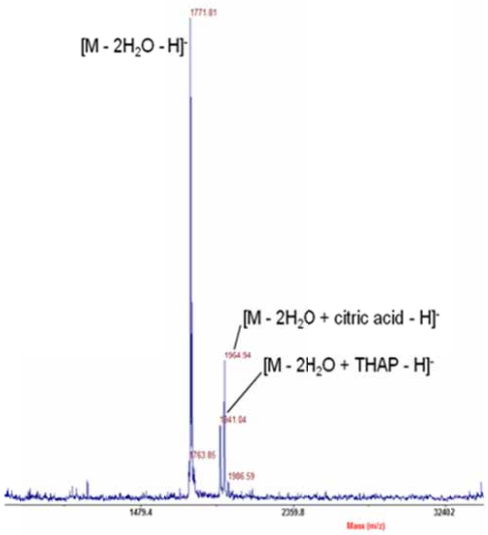

MALDI-TOF MS conditions analysis: ionization in negative mode THAP (MW= 168.15 g.mol^{-1}) as matrix and ammonium citrate (MW= 243.2 g.mol^{-1}) as co-matrix, delay time 100 ns and an acceleration voltage of 24 kV.

HPLC and MALDI-TOF analysis of 5'-T^{bn}TTTTTT-3'

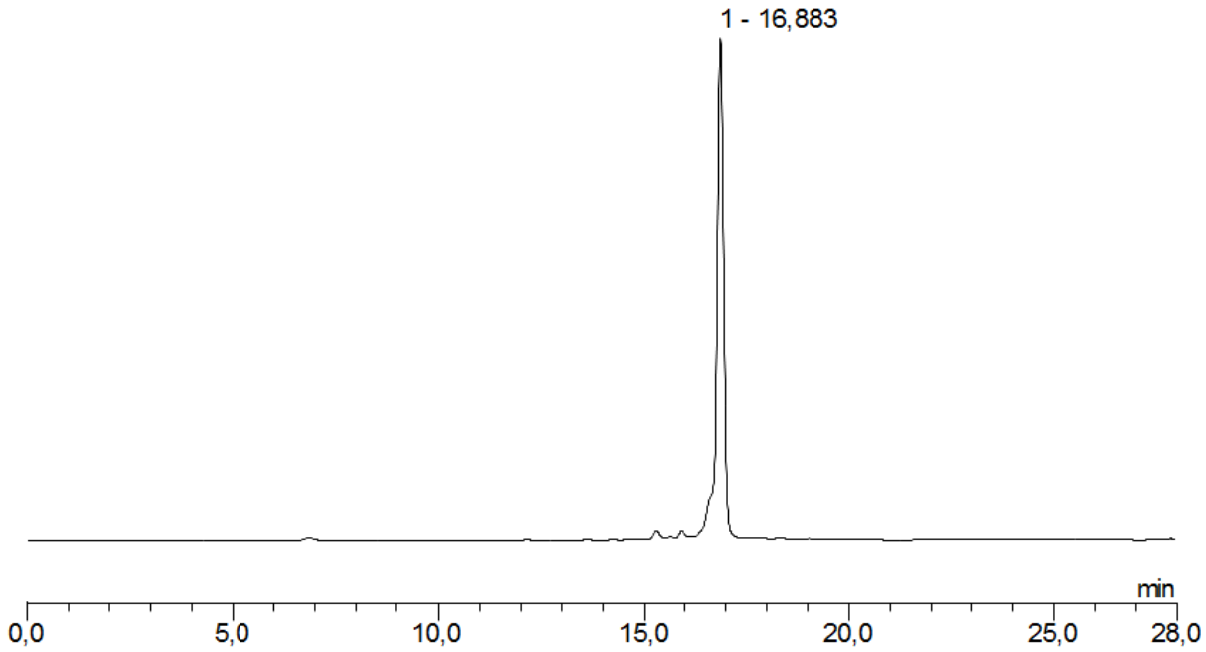

HPLC conditions analysis: Column Nucleodur C18, 100 Å, 3 µm, elution with a linear gradient of 0 to 20% CH_3CN in triethylammonium acetate buffer, pH 7, in 25min, Flow rate 1 mL.min^{-1}, λ 260 nm.

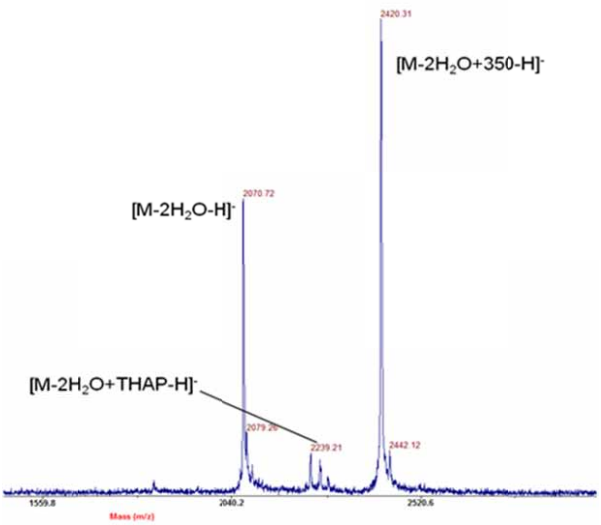

MALDI-TOF MS conditions analysis: ionization in negative mode, THAP (MW= 168.15 g.mol^{-1}) as matrix and ammonium citrate (MW= 243.2 g.mol^{-1}) as co-matrix, delay time 150 ns and an acceleration voltage of 24 kV.

*HPLC and MALDI-TOF analysis of 5'-T^{bn}CAGC**G**-3'*

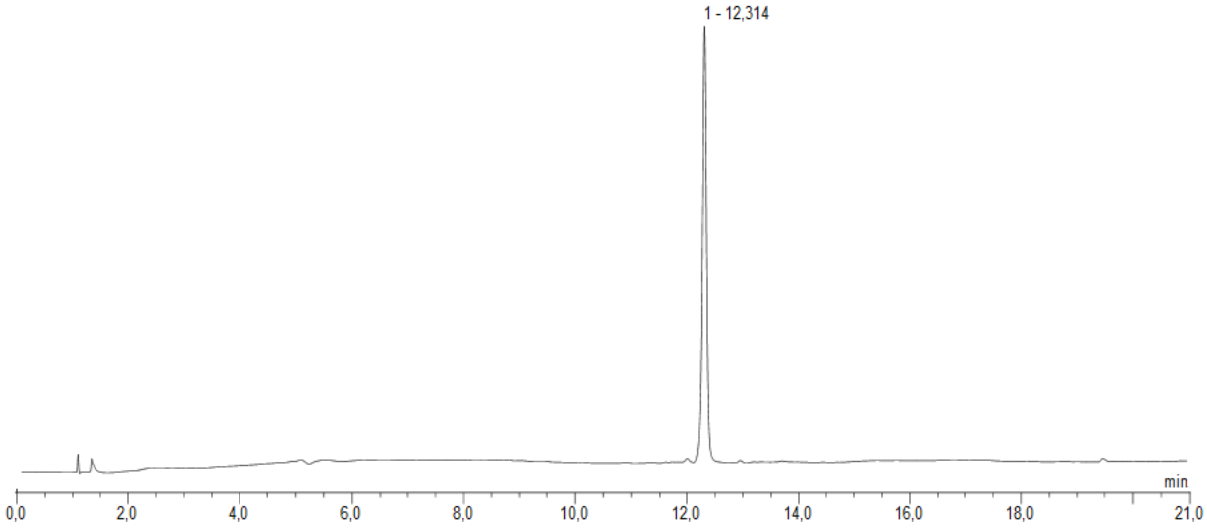

HPLC conditions analysis: Column Nucleodur C18, 100 Å, 3 µm, elution with a linear gradient of 0 to 20% CH_3CN in triethylammonium acetate buffer, pH 7, in 20min, Flow rate 1 mL.min^{-1}, λ 260 nm.

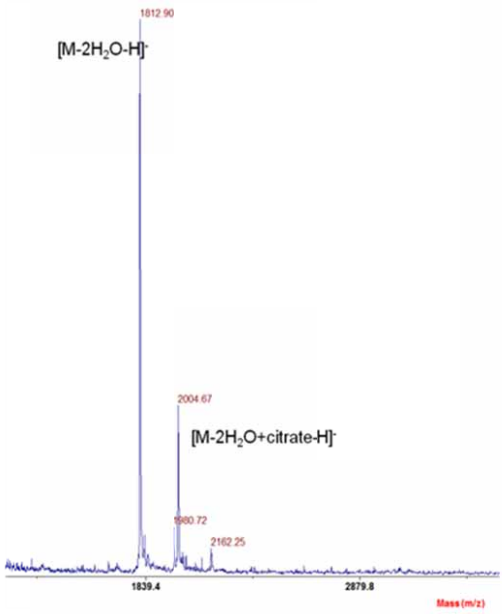

MALDI-TOF MS conditions analysis: ionization in negative mode, THAP (MW= 168.15 g.mol^{-1}) as matrix and ammonium citrate (MW= 243.2 g.mol^{-1}) as co-matrix, delay time 150 ns and an acceleration voltage of 24 kV.

*HPLC and MALDI-TOF analysis of 5'-T^{bn}GACG**C**-3'*

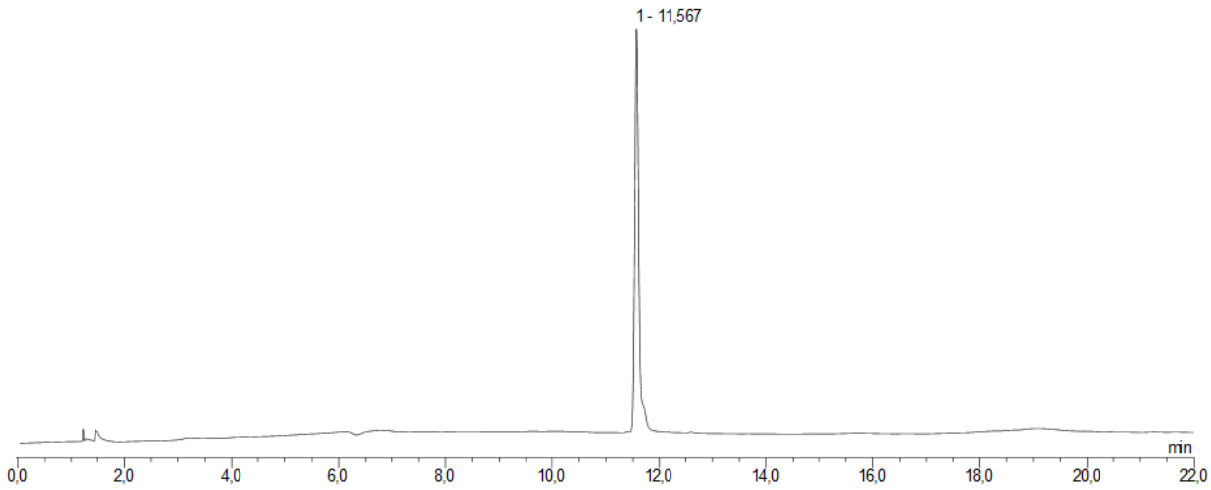

HPLC conditions analysis: Column Nucleodur C18, 100 Å, 3 µm, elution with a linear gradient of 0 to 20% CH_3CN in triethylammonium acetate buffer, pH 7, in 20min, Flow rate 1 mL.min^{-1}, λ 260 nm.

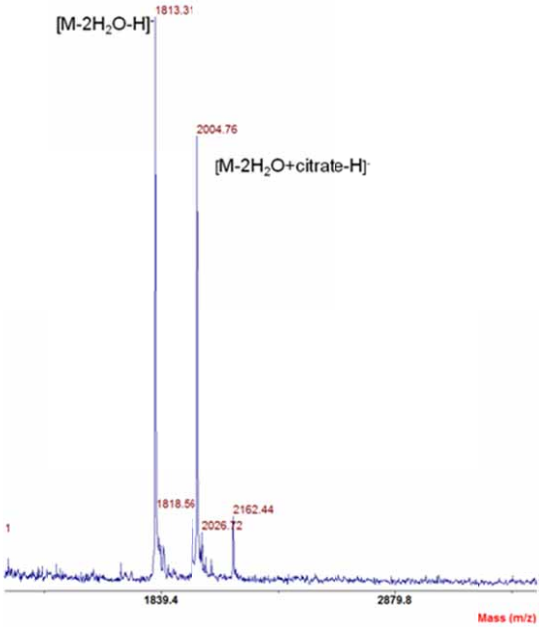

MALDI-TOF MS conditions analysis: ionization in negative mode, THAP (MW= 168.15 g.mol^{-1}) as matrix and ammonium citrate (MW= 243.2 g.mol^{-1}) as co-matrix, delay time 150 ns and an acceleration voltage of 24 kV.

Denaturation experiments

Unless otherwise stated, the samples were prepared by mixing 3 µM of the template with stoichiometric amounts of complementary strands. Denaturation experiments were performed in a 1M NaCl, 10mM sodium cacodylate buffer at pH 7.5, 8.5 or 9.5. A heating-cooling-heating cycle in the 0-90°C temperature range with a gradient of 0.5°C/min was applied.

Tm values were determined from the maxima of the first derivative plots of absorbance at 260 nm versus temperature.

Melting curves and their derivatives

Melting curves and derivatives from Table 1.

Table 1, entry 1 :

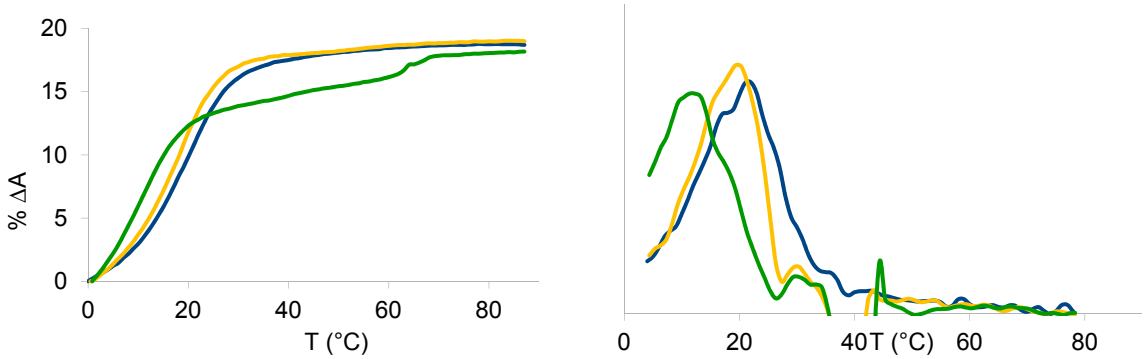

Melting curves and their derivatives of the complex 3'-CC(ACACAT)$_2$CC/5'-TGTGTrA at pH 7.5 (blue) ; pH 9.5 (orange) ; pH 7.5 3mM CN^- (green).

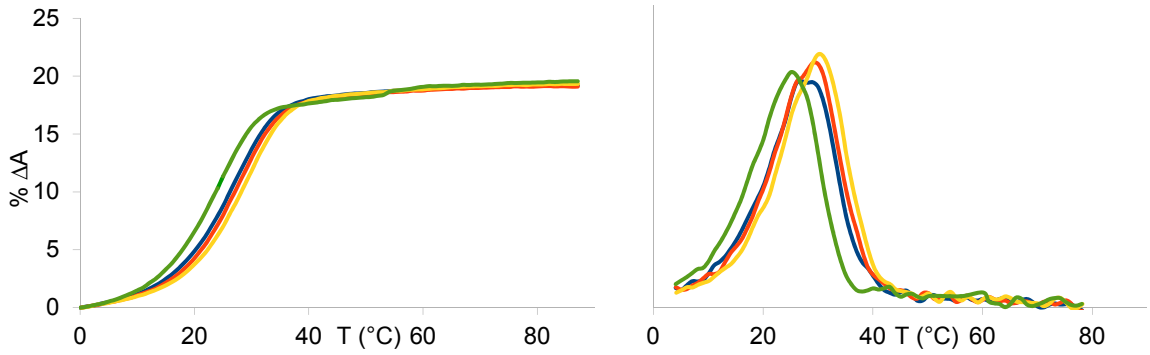

Melting curves and their derivatives of the complex 3'-CC(ACACAT)$_2$CC/5'-T^{bn}GTGTrA at pH 7.5 (blue) ; pH 8.5 (orange) ; pH 9.5 (yellow) and pH 7.5 3mM CN^- (green).

Table 1, entry 2 :

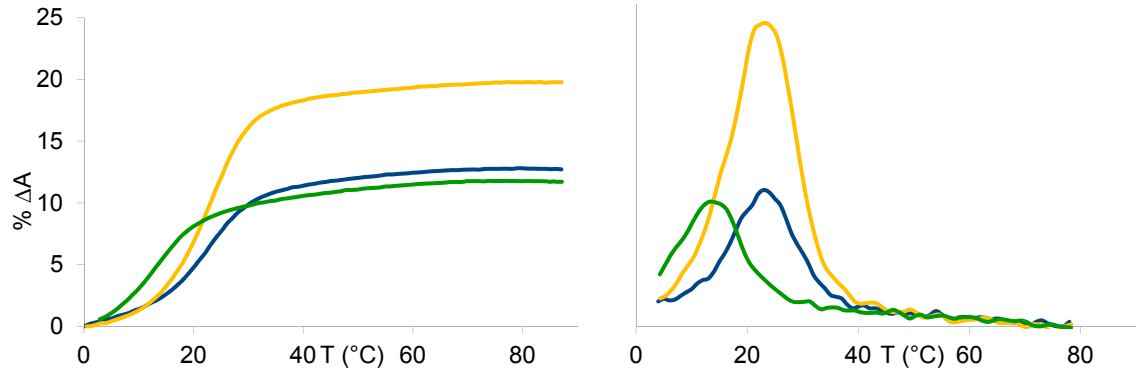

Melting curves and their derivatives of the complex 3'-CC(ACACAT)$_3$CC/5'-TGTGTrA at pH 7.5 (blue) ; pH 9.5 (yellow) ; pH 7.5 3mM CN^- (green).

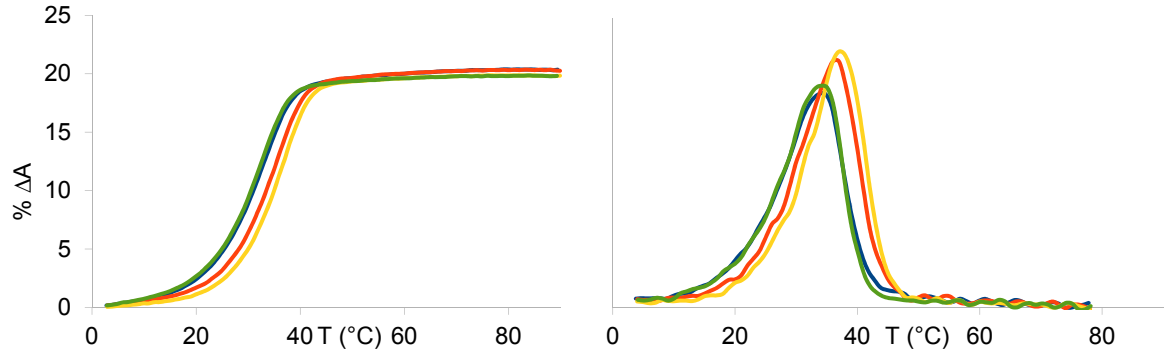

Melting curves and their derivatives of the complex 3'-CC(ACACAT)$_3$CC/5'-T^{bn}GTGTrA at pH 7.5 (blue) ; pH 8.5 (orange) ; pH 9.5 (yellow) and pH 7.5 3mM CN^- (green).

Table 1, entry 3 :

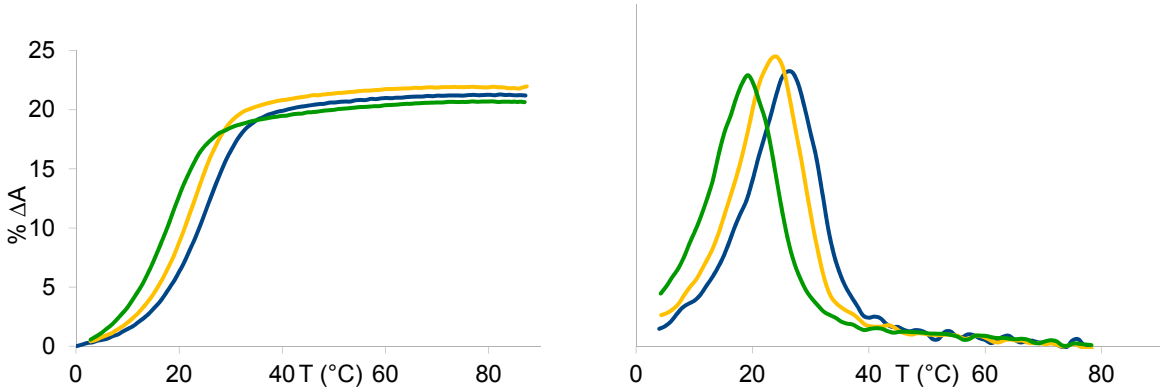

Melting curves and their derivatives of the complex 3'-CC(ACACAT)$_4$CC/5'-TGTGTrA at pH 7.5 (blue) ; pH 9.5 (yellow) ; pH 7.5 3mM CN^- (green).

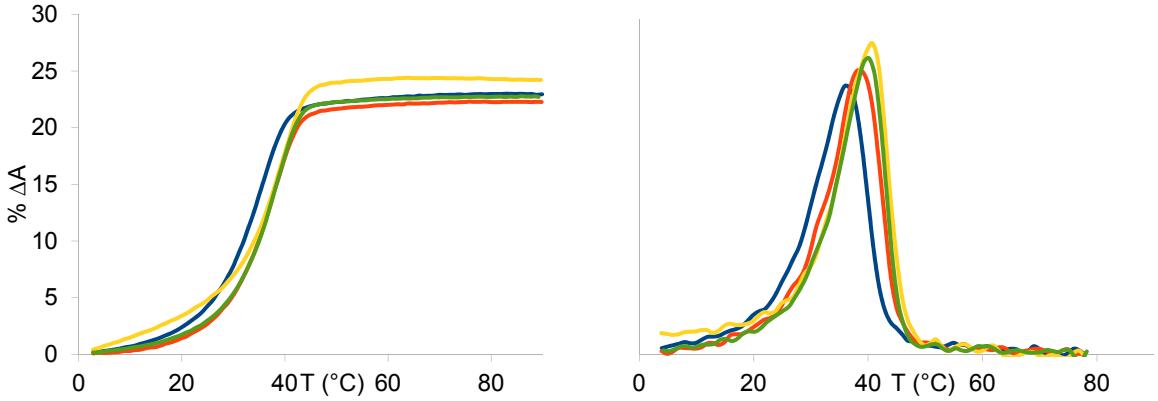

Melting curves and their derivatives of the complex 3'-CC(ACACAT)$_4$CC/5'-T^{bn}GTGTrA at pH 7.5 (blue) ; pH 8.5 (orange) ; pH 9.5 (yellow) and pH 7.5 3mM CN^- (green).

Table 1, entry 4 :

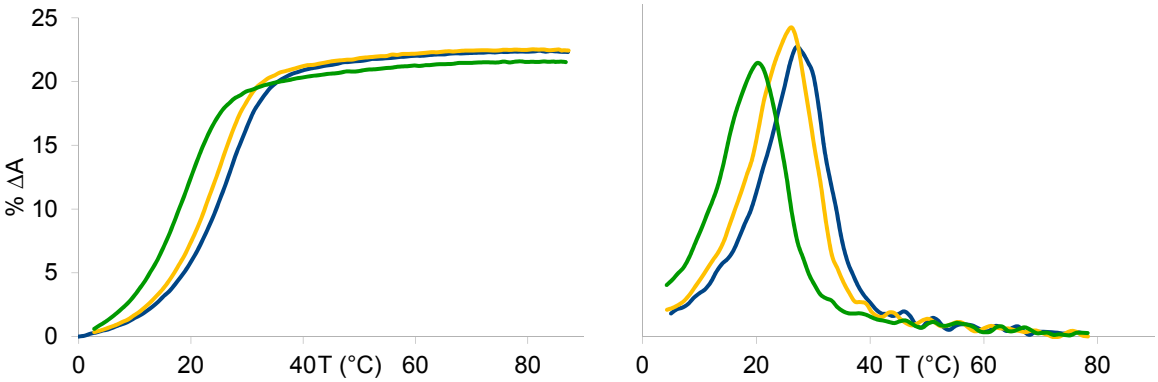

Melting curves and their derivatives of the complex 3'-CC(ACACAT)$_5$CC/5'-TGTGTrA at pH 7.5 (blue) ; pH 9.5 (yellow) ; pH 7.5 3mM CN^- (green).

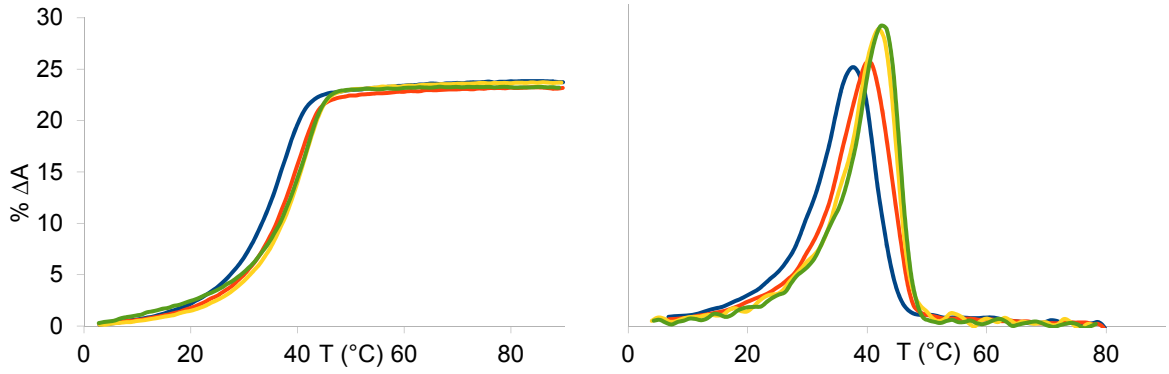

Melting curves and their derivatives of the complex 3'-CC(ACACAT)$_5$CC/5'-T^{bn}GTGTrA at pH 7.5 (blue) ; pH 8.5 (orange) ; pH 9.5 (yellow) and pH 7.5 3mM CN^- (green).

Table 1, entry 5 :

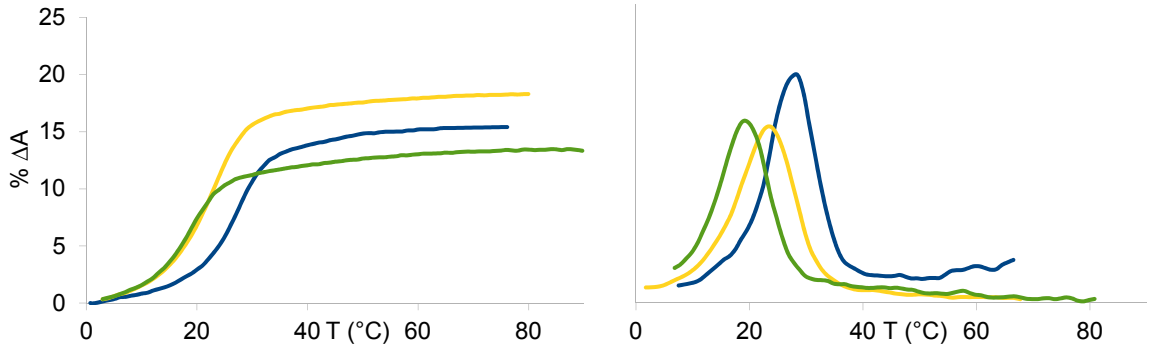

Melting curves and their derivatives of the complex 3'-CC(ACACAT)$_6$CC/5'-TGTGTrA at pH 7.5 (blue) ; pH 9.5 (yellow) ; pH 7.5 3mM CN^- (green).

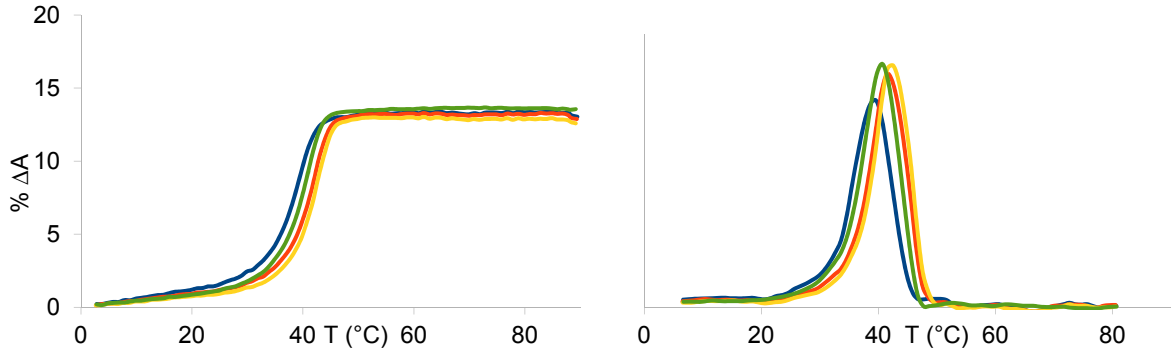

Melting curves and their derivatives of the complex 3'-CC(ACACAT)$_6$CC/5'-T^{bn}GTGTrA at pH 7.5 (blue) ; pH 8.5 (orange) ; pH 9.5 (yellow) and pH 7.5 3mM CN^- (green).

Table 1, entry 6 :

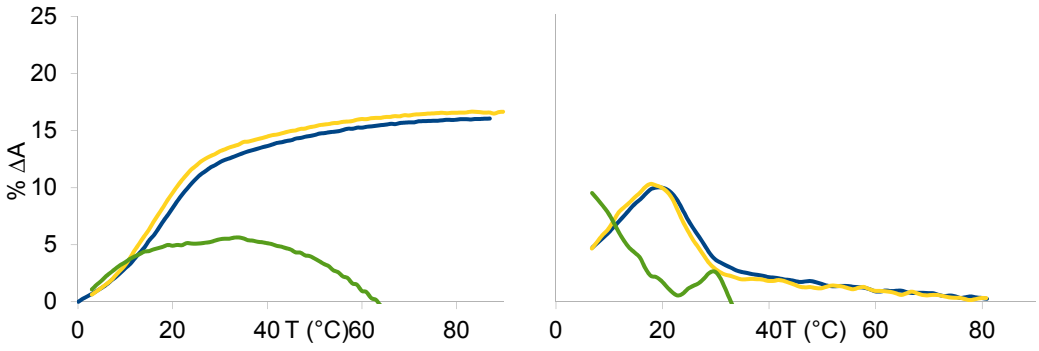

Melting curves and their derivatives of the complex 3'-r(CC(ACACAU)$_2$CC)/5'-TGTGTrA at pH 7.5 (blue) ; pH 9.5 (yellow) ; pH 7.5 3mM CN^- (green).

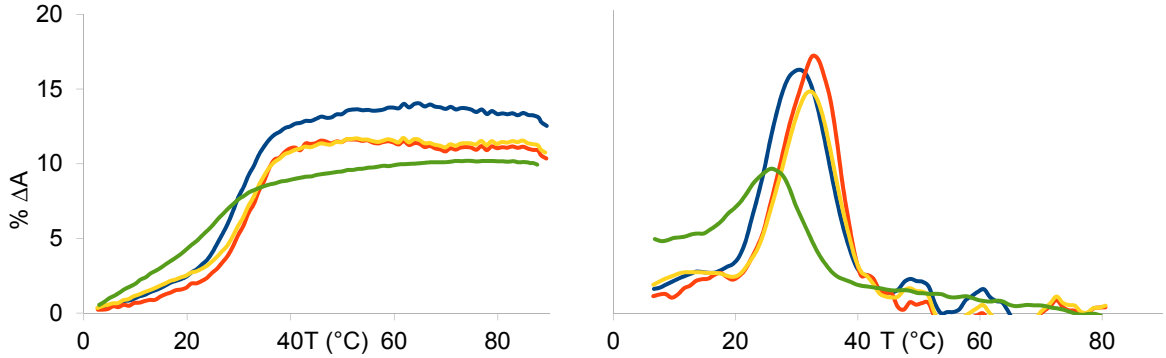

Melting curves and their derivatives of the complex 3'-r(CC(ACACAU)$_2$CC)/5'-T^{bn}GTGTrA at pH 7.5 (blue) ; pH 8.5 (orange) ; pH 9.5 (yellow) and pH 7.5 3mM CN^- (green).

Table 1, entry 7 :

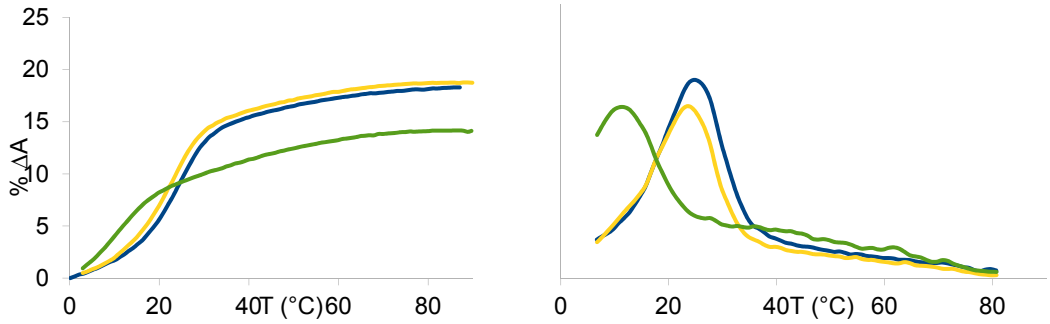

Melting curves and their derivatives of the complex 3'-r(CC(ACACAU)$_3$CC)/5'-TGTGTrA at pH 7.5 (blue) ; pH 9.5 (yellow) ; pH 7.5 3mM CN^- (green).

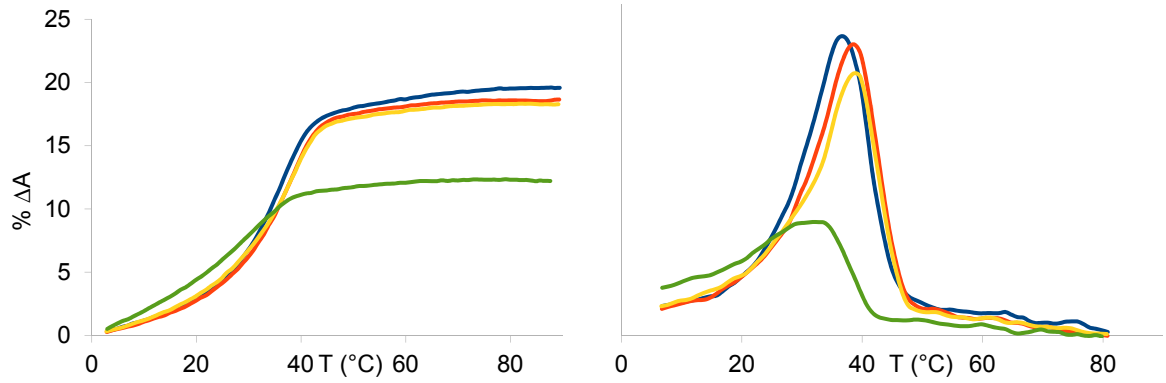

Melting curves and their derivatives of the complex 3'-r(CC(ACACAU)$_3$CC)/5'-T^{bn}GTGTrA at pH 7.5 (blue) ; pH 8.5 (orange) ; pH 9.5 (yellow) and pH 7.5 3mM CN^- (green).

Table 1, entry 8 :

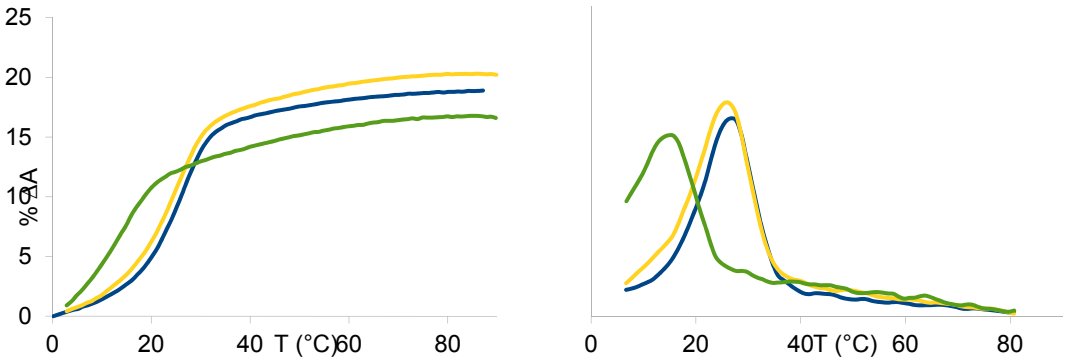

Melting curves and their derivatives of the complex 3'-r(CC(ACACAU)$_4$CC)/5'-TGTGTrA at pH 7.5 (blue) ; pH 9.5 (yellow) ; pH 7.5 3mM CN^- (green).

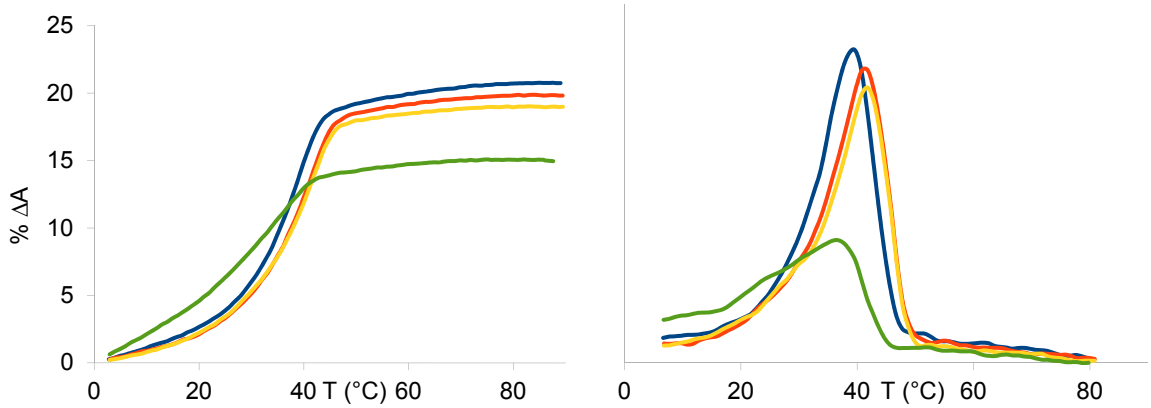

Melting curves and their derivatives of the complex 3'-r(CC(ACACAU)$_4$CC)/5'-T^{bn}GTGTrA at pH 7.5 (blue) ; pH 8.5 (orange) ; pH 9.5 (yellow) and pH 7.5 3mM CN^- (green).

Table 1, entry 9 :

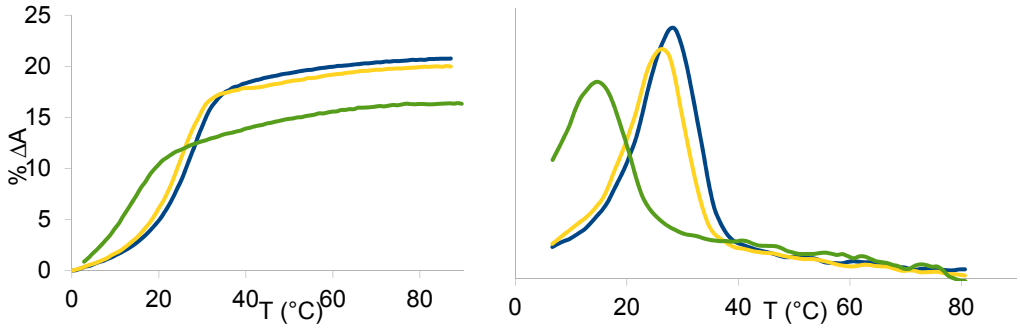

Melting curves and their derivatives of the complex 3'-r(CC(ACACAU)$_5$CC)/5'-TGTGTrA at pH 7.5 (blue) ; pH 9.5 (yellow) ; pH 7.5 3mM CN^- (green).

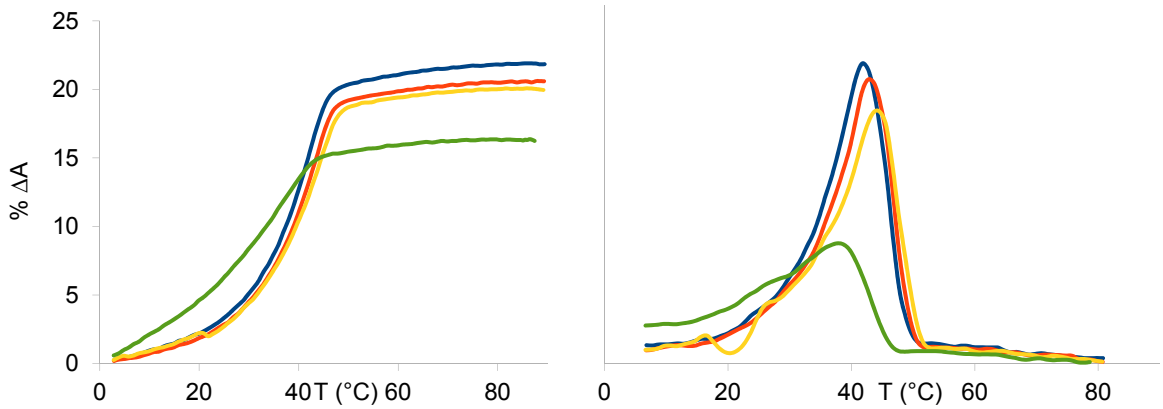

Melting curves and their derivatives of the complex 3'-r(CC(ACACAU)$_5$CC)/5'-T^{bn}GTGTrA at pH 7.5 (blue) ; pH 8.5 (orange) ; pH 9.5 (yellow) and pH 7.5 3mM CN^- (green).

Melting curves and derivatives from Table 2.

Table 2, entry 1 :

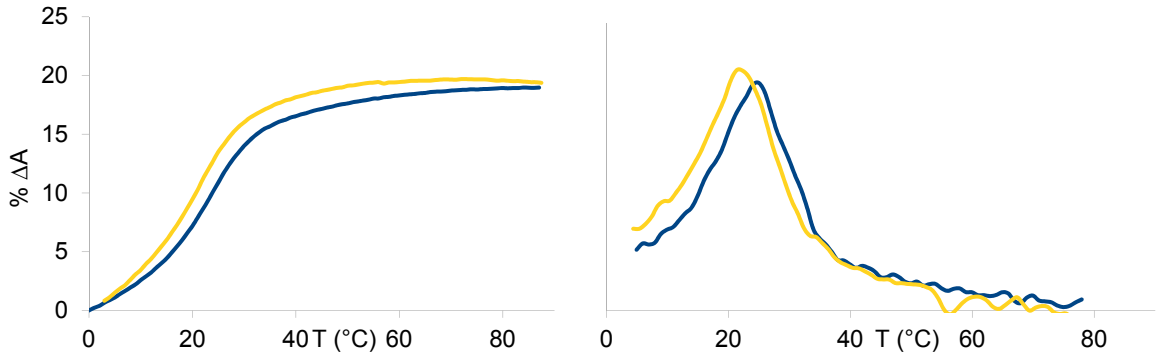

Melting curves and their derivatives of the complex 3'-CC-(ACACAT)$_2$-AGTAGT-(ACACAT)$_2$-CC / 5'-TGTGTrA (1/4) at pH 7.5 (blue) and pH 9.5 (yellow).

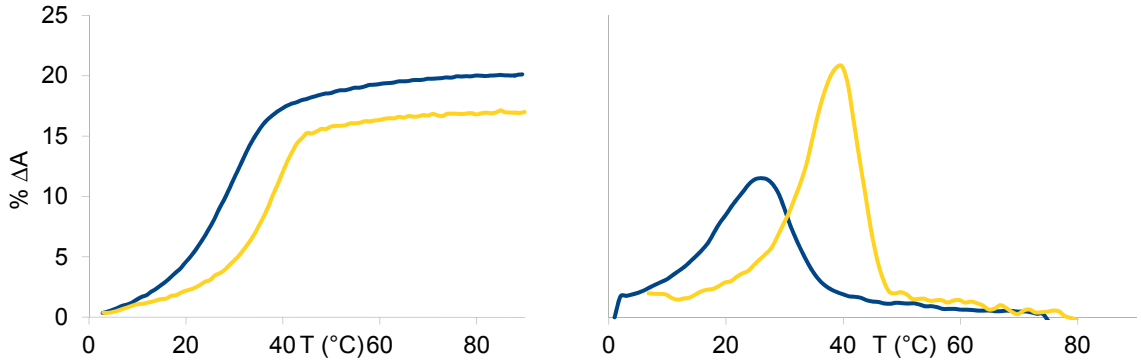

Melting curves and their derivatives of the complex 3'-CC-(ACACAT)$_2$-AGTAGT-(ACACAT)$_2$-CC / 5'-T^{bn}GTGTrA (1/4) at pH 7.5 (blue) and pH 9.5 (yellow).

Table 2, entry 2 :

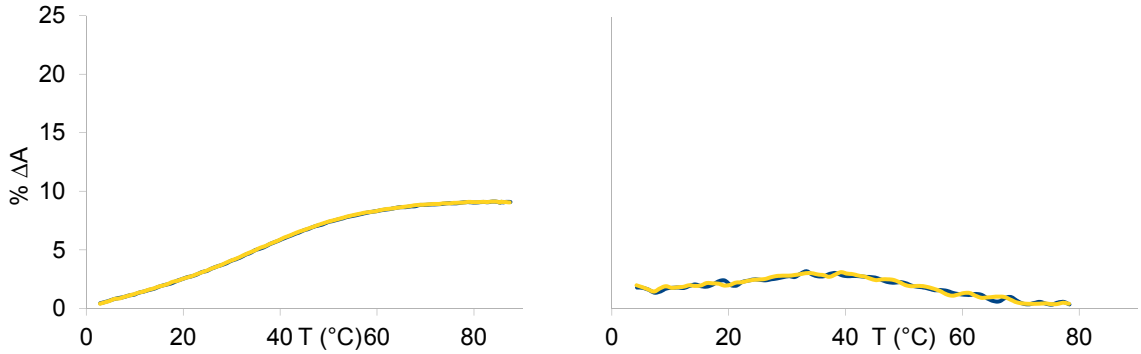

Melting curves and their derivatives of the complex 3'-CC-(ACACAT)$_2$-AGTAGT-(ACACAT)$_2$-CC / 5'-TCATCrA (1/1) equiv at pH 7.5 (blue) and pH 9.5 (yellow).

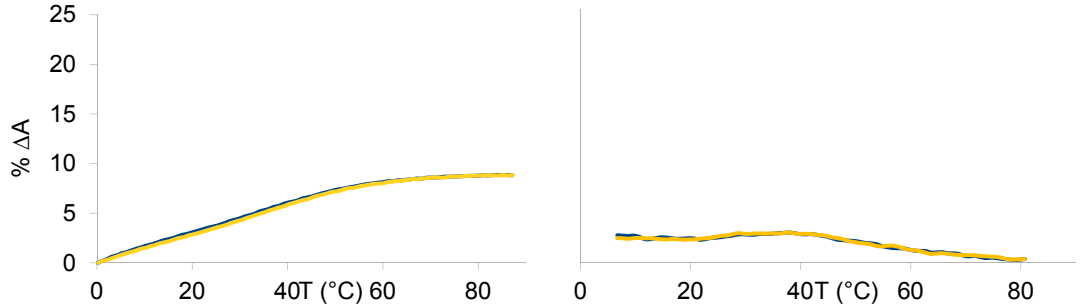

Melting curves and their derivatives of the complex 3'-CC-(ACACAT)$_2$-AGTAGT-(ACACAT)$_2$-CC / 5'-T^{bn}CATCrA (1/1) equiv at pH 7.5 (blue) and pH 9.5 (yellow).

Table 2, entry 3 :

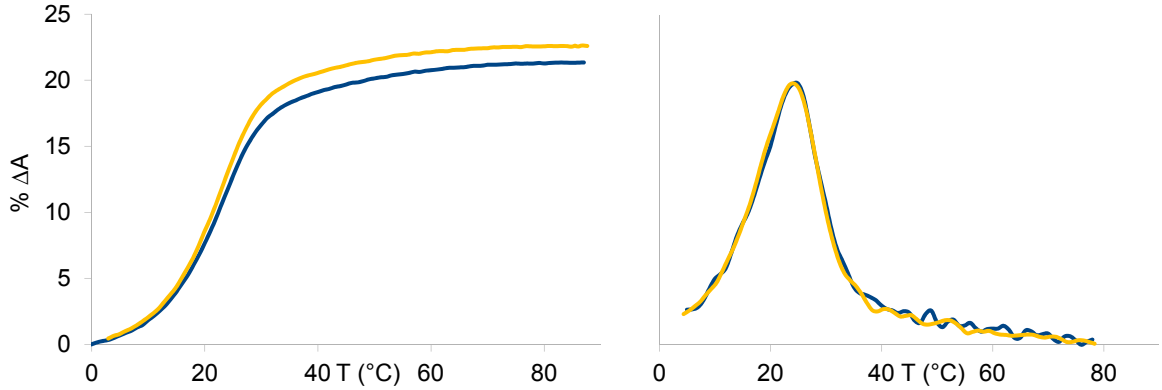

Melting curves and their derivatives of the complex 3'-CC(ACACAT)$_2$-AGTAGT-(ACACAT)$_2$-CC / 5'-TGTGTrA / 5'-TCATCrA (1/4/1) and pH 9.5 (yellow).

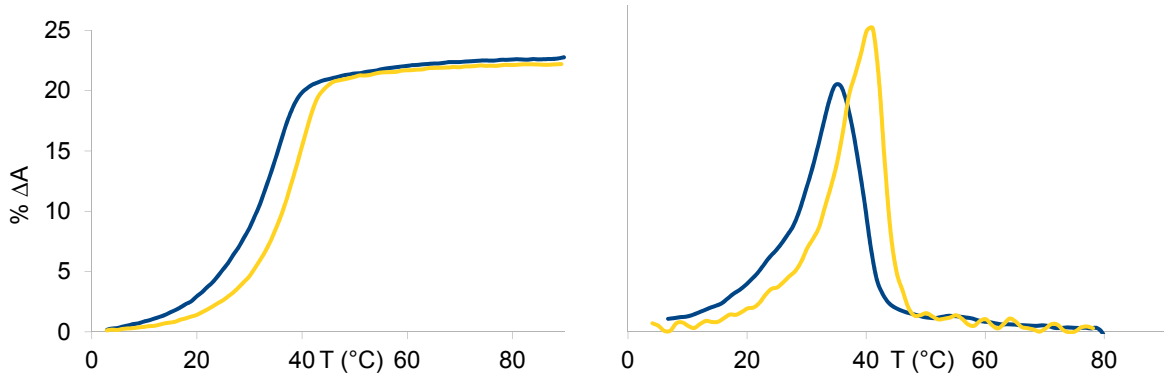

Melting curves and their derivatives of the complex 3'-CC(ACACAT)$_2$-AGTAGT-(ACACAT)$_2$-CC / 5'-T^{bn}GTGTrA / 5'-T^{bn}CATCrA (1/4/1) at pH 7.5 (blue) and pH 9.5 (yellow).

Table 2, entry 4 :

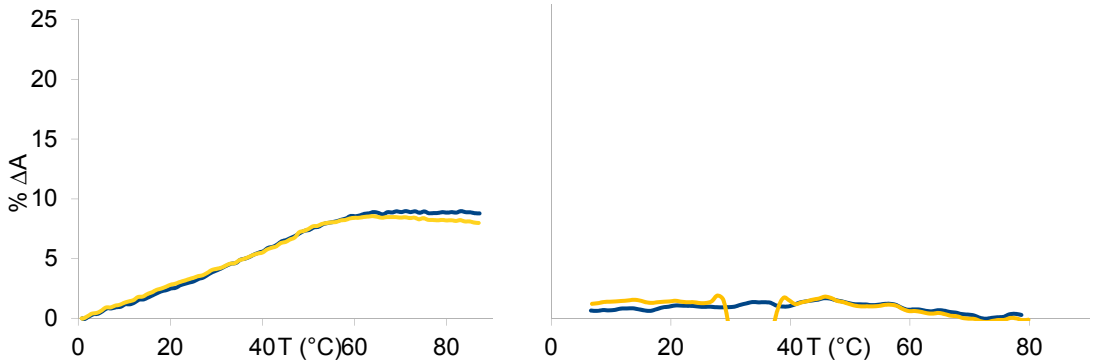

Melting curves and their derivatives of the complex 3'-CC-AGTAGT-(ACACAT-AGTAGT)$_2$-CC / 5'-TGTGTrA (1/2) at pH 7.5 (blue) and pH 9.5 (yellow).

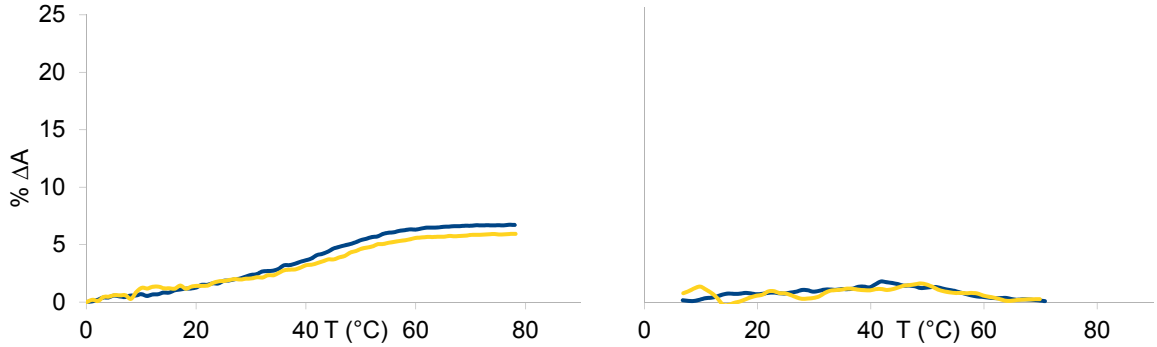

Melting curves and their derivatives of the complex 3'-CC-AGTAGT-(ACACAT-AGTAGT)$_2$-CC / 5'-T^{bn}GTGTrA (1/2) at pH 7.5 (blue) and pH 9.5 (yellow).

Table 2, entry 5 :

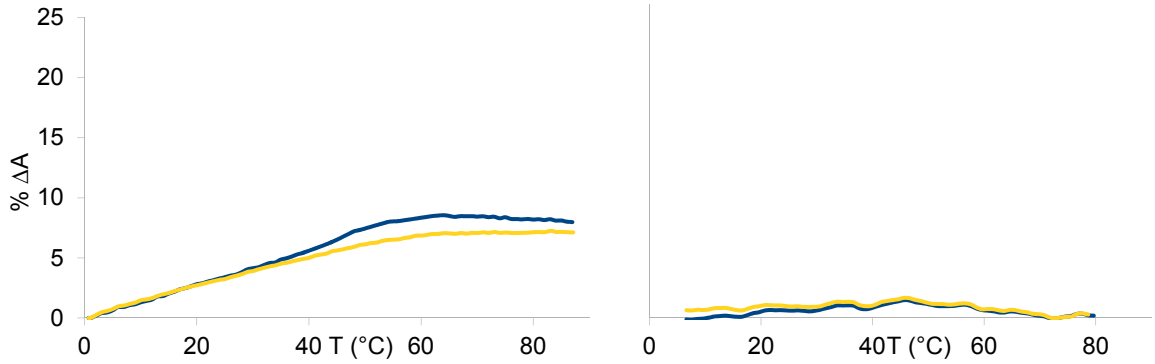

Melting curves and their derivatives of the complex 3'-CC-AGTAGT-(ACACAT-AGTAGT)$_2$-CC / 5'-TCATCrA (1/3) at pH 7.5 (blue) and pH 9.5 (yellow).

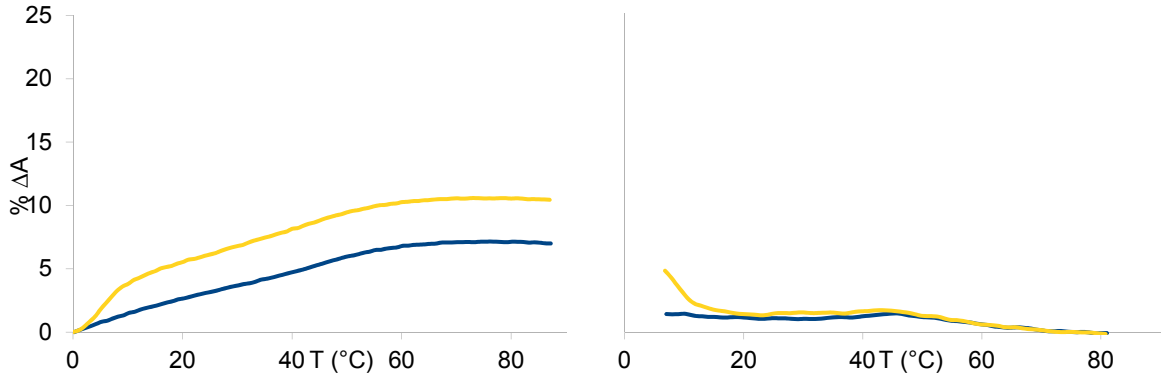

Melting curves and their derivatives of the complex 3'-CC-AGTAGT-(ACACAT-AGTAGT)$_2$-CC / 5'-T^{bn}CATCrA (1/3) at pH 7.5 (blue) and pH 9.5 (yellow).

Table 2, entry 6 :

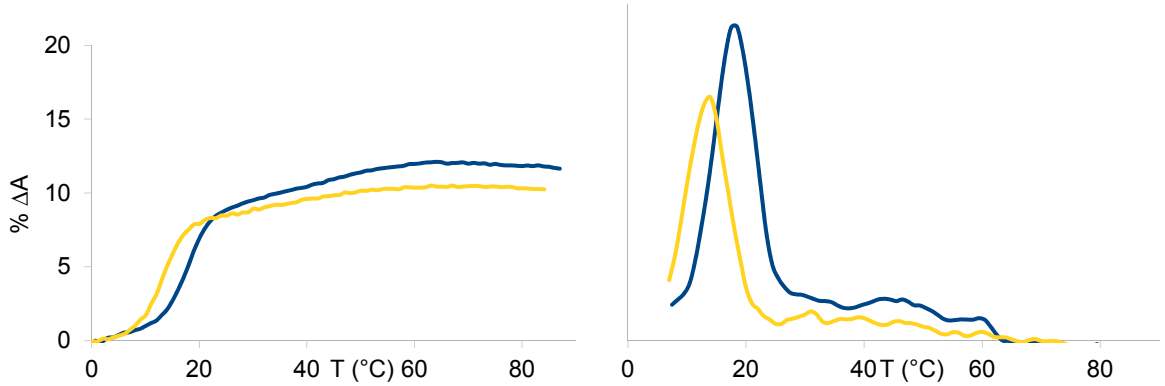

Melting curves and their derivatives of the complex 3'-CC-AGTAGT-(ACACAT-AGTAGT)$_2$-CC / 5'-TGTGTrA / 5'-TCATCrA (1/2/3) at pH 7.5 (blue) ; pH 9.5 (yellow).

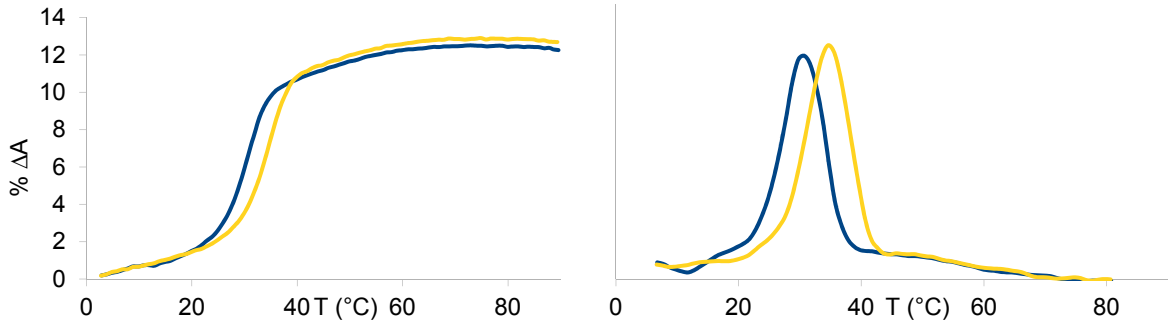

Melting curves and their derivatives of the complex 3'-CC CCAGTAGT-(ACACAT-AGTAGT)$_2$-CC / 5'-T^{bn}GTGTrA / 5'-T^{bn}CATCrA (1/2/3) at pH 7.5 (blue) ; pH 9.5 (yellow).

Table 2, entry 7 :

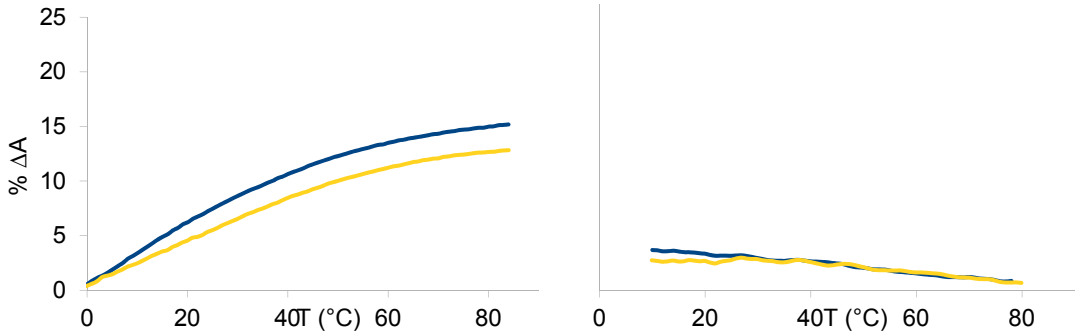

Melting curves and their derivatives of the complex 3'-CC-AGTAGT-ACACAT-AAAAAAA-CC / 5'-TCATCrA (1/1) at pH 7.5 (blue) and pH 9.5 (yellow).

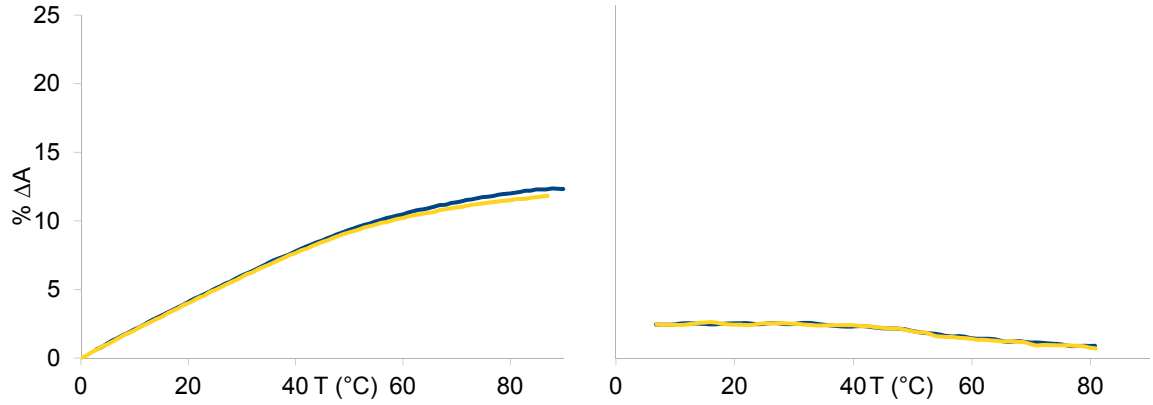

Melting curves and their derivatives of the complex 3'-CC-AGTAGT-ACACAT-AAAAAAA-CC / 5'-T^{bn}CATCrA (1/1) at pH 7.5 (blue) and pH 9.5 (yellow).

Table 2, entry 8 :

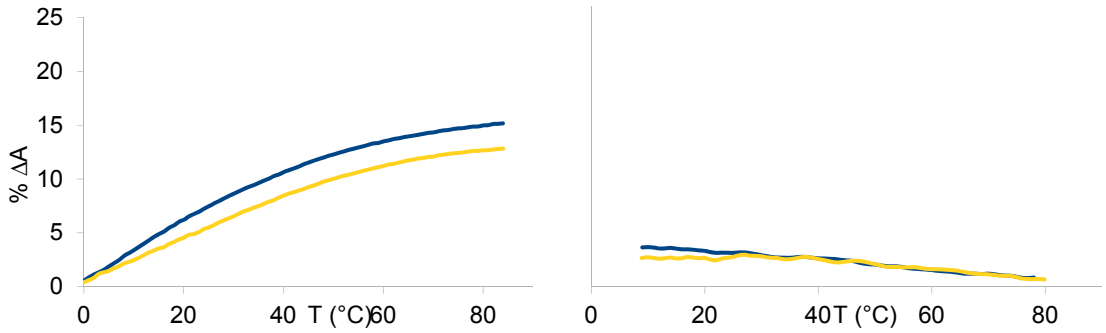

Melting curves and their derivatives of the complex 3'-CC-AGTAGT-ACACAT-AAAAAAA-CC /5'-TGTGTrA (1/1) at pH 7.5 (blue) and pH 9.5 (yellow).

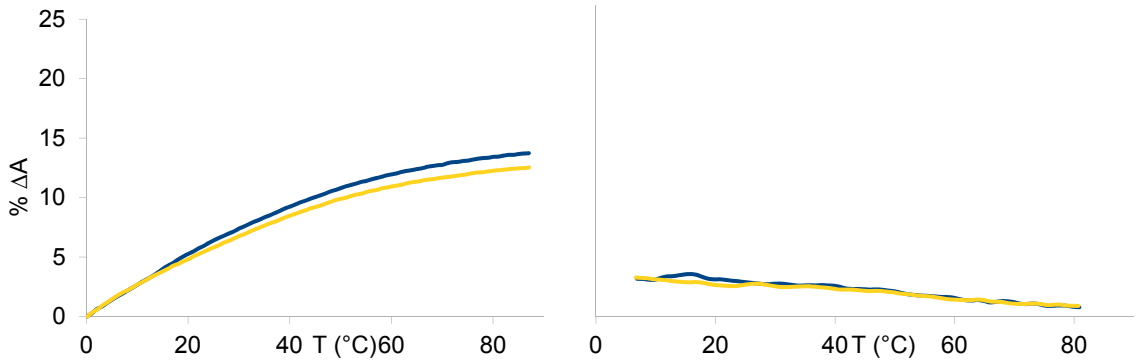

Melting curves and their derivatives of the complex 3'-CC-AGTAGT-ACACAT-AAAAAAA-CC /5'-T^{bn}GTGTrA (1/1) at pH 7.5 (blue) and pH 9.5 (yellow).

Table 2, entry 9 :

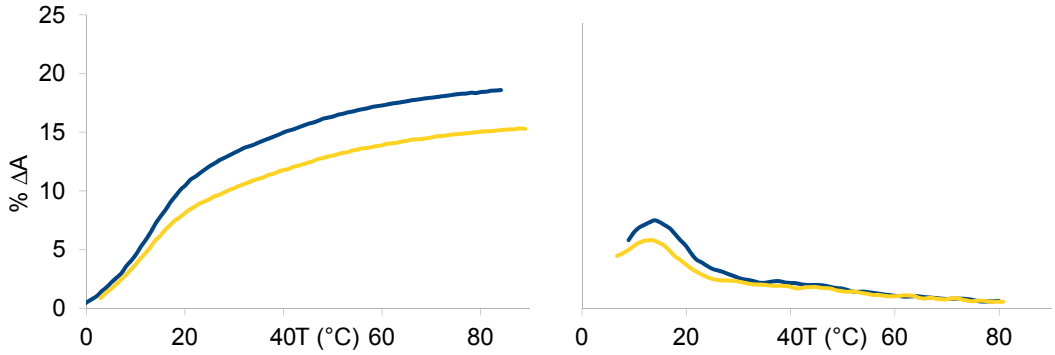

Melting curves and their derivatives of the complex 3'-CC-AGTAGT-ACACAT-AAAAAAA-CC /5'-T_7 (1/1) at pH 7.5 (blue) and pH 9.5 (yellow).

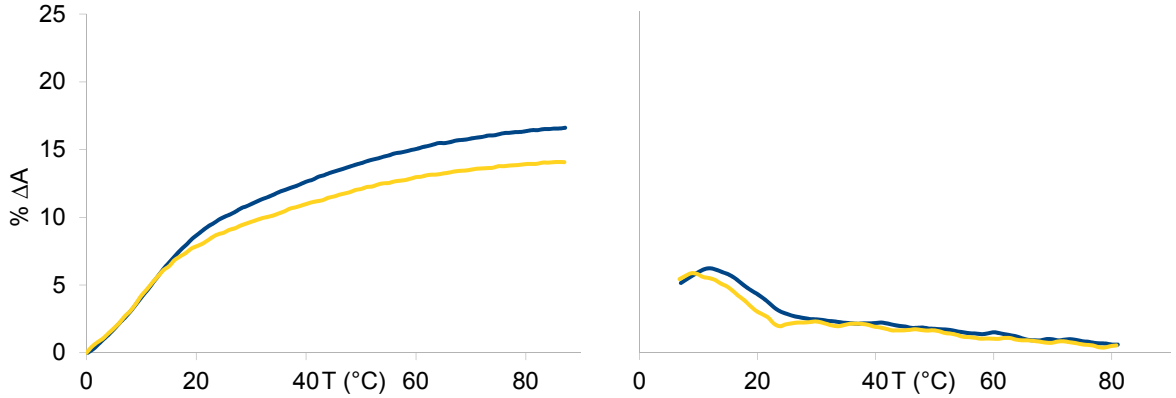

Melting curves and their derivatives of the complex 3'-CC-AGTAGT-ACACAT-AAAAAAA-CC /5'-T^{bn}T$_6$ (1/1) at pH 7.5 (blue) and pH 9.5 (yellow).

Table 2, entry 10 :

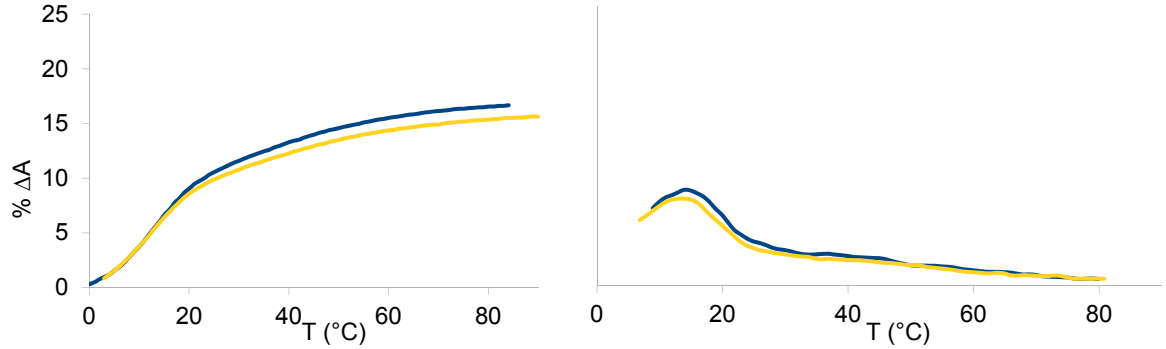

Melting curves and their derivatives of the complex 3'-CC-AGTAGT-ACACAT-AAAAAAA-CC /5'-TGTGTrA / 5'-TCATCrA (1/1/1) at pH 7.5 (blue) and pH 9.5 (yellow).

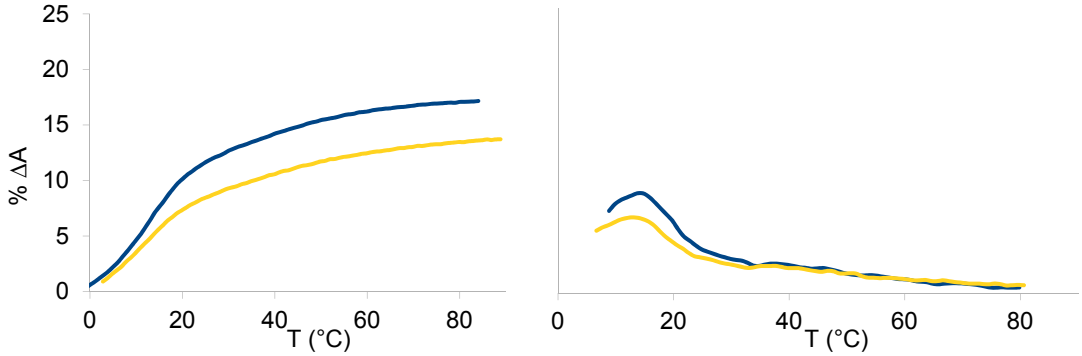

Melting curves and their derivatives of the complex 3'-CC-AGTAGT-ACACAT-AAAAAAA-CC /5'-T^{bn}GTGTrA / 5'-T^{bn}CATCrA (1/1/1) at pH 7.5 (blue) and pH 9.5 (yellow).

Table 2, entry 11 :

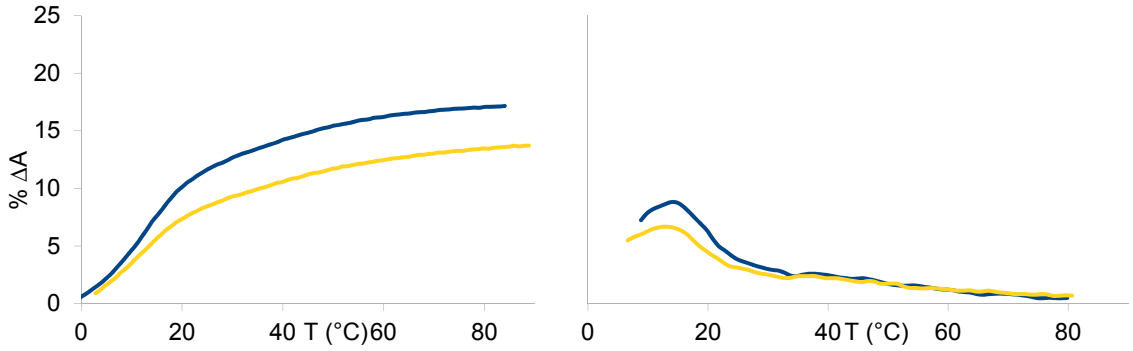

Melting curves and their derivatives of the complex 3'-CC-AGTAGT-ACACAT-AAAAAAA-CC /5'-TCATCrA / 5'-T_7 (1/1/1) at pH 7.5 (blue) and pH 9.5 (yellow).

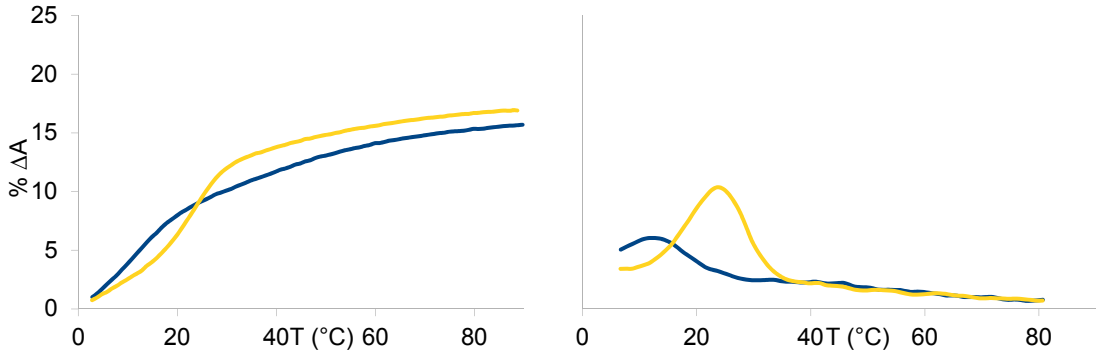

Melting curves and their derivatives of the complex 3'-CC-AGTAGT-ACACAT-AAAAAAA-CC /5'-T^{bn}CATCrA / 5'-$T^{bn}T_6$ (1/1/1) at pH 7.5 (blue) and pH 9.5 (yellow).

Table 2, entry 12 :

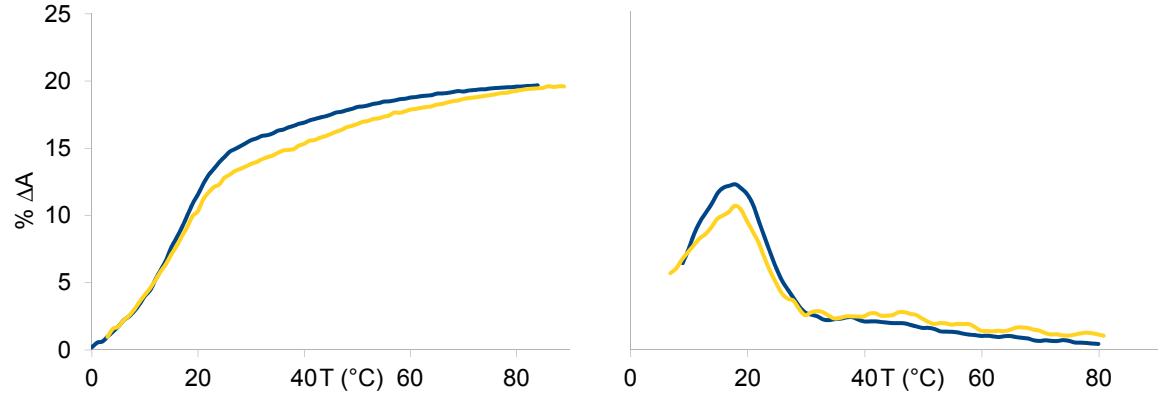

Melting curves and their derivatives of the complex 3'-CC-AGTAGT-ACACAT-AAAAAAA-CC /5'-TGTGTrA / 5'-T_7 (1/1/1) at pH 7.5 (blue) and pH 9.5 (yellow).

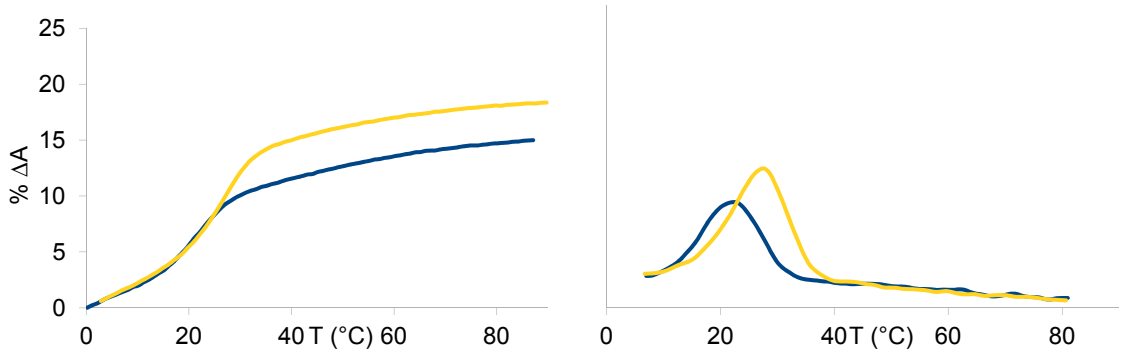

Melting curves and their derivatives of the complex 3'-CC-AGTAGT-ACACAT-AAAAAAA-CC /5'-T^{bn}GTGTrA / 5'-T^{bn}T$_6$ (1/1/1) at pH 7.5 (blue) and pH 9.5 (yellow).

Table 2, entry 13 :

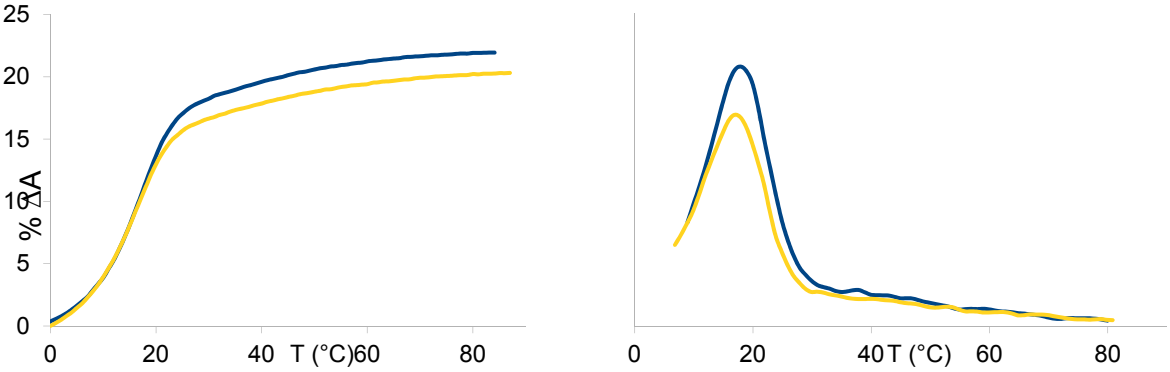

Melting curves and their derivatives of the complex 3'-CCAGTAGT-ACACAT-AAAAAAA-CC/5'-TGTGTrA/5'-TCATCrA/5'-T$_7$ (1/1/1/1) at pH 7.5 (blue) ; pH 9.5 (yellow).

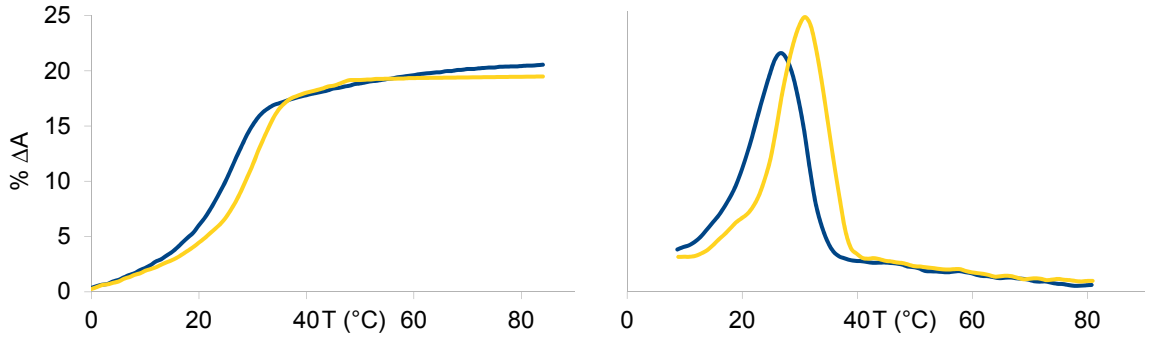

Melting curves and their derivatives of the complex 3'-CC-AGTAGT-ACACAT-AAAAAAA-CC /5'-T^{bn}GTGTrA/5'-T^{bn}CATCrA/5'-T^{bn}T$_6$ (1/1/1/1) at pH 7.5 (blue) ; pH 9.5 (yellow).

Assembly along templates having alternative sections with cyanide anions.

Table S2. UV thermal denaturation data with templates having alternative sections at pH 7.5 with cyanide anions.

Entry	Template	Complementary units	T_m [°C][a]
1	3'-CC $(ACACAT)_2$ AGTAGT $(ACACAT)_2$ CC	C_1 / C_2	18.2
		B_1 / B_2	41.0
2	3'-CC AGTAGT $(ACACAT\ AGTAGT)_2$ CC	C_1 / C_2	8.0
		B_1 / B_2	33.8
3	3'-CC AGTAGT ACACAT AAAAAAA CC	C_1 / C_2 / C_3	17.9
		B_1 / B_2 / B_3	30.8

[a]Melting temperatures are obtained from the maxima of the first derivatives of the melting curve (A260 vs temperature) recorded in a buffer containing 1 M NaCl and 10 mM of sodium cacodylate at pH 7.5 and 3 mM sodium cyanide, Template concentration 3 µM; C_n and B_n concentrations were adjusted according to stoichiometry. [b]B_n refer to 5'-TbnGTGTrA (B_1), 5'-T^{bn}CATCrA (B_2) and 5'-T^{bn}TTTTTT (B_3) ; C_1, C_2 and C_3 refer to their corresponding unmodified analogues.

Table S2, entry 1 :

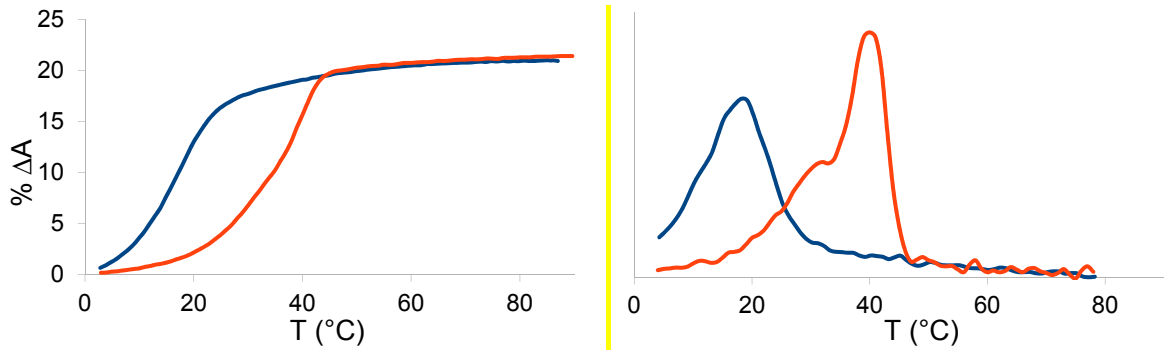

Melting curves and their derivatives of the template 3'-CC $(ACACAT)_2$ AGTAGT $(ACACAT)_2$ CC with 5'-TGTGTrA / 5'-TCATCrA (blue) or 5'-T^{bn}GTGTrA / 5'-T^{bn}CATCrA (orange) at pH 7.5 3mM CN^-.

Table S2, entry 2 :

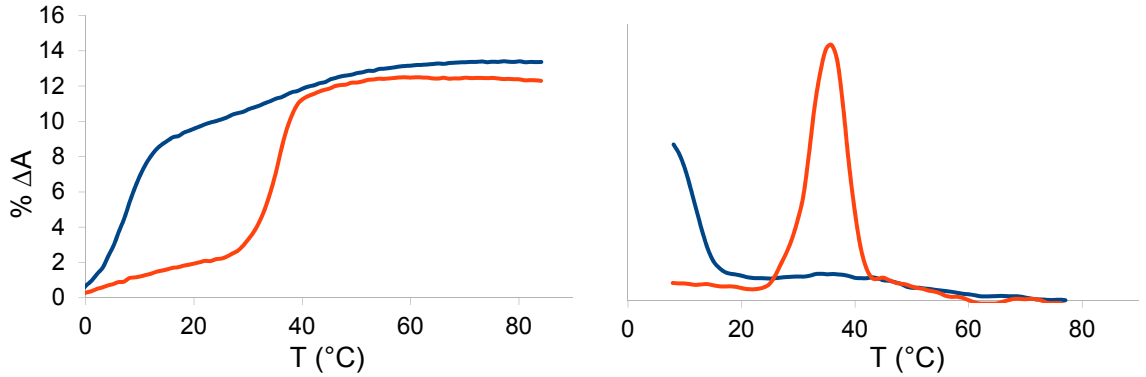

Melting curves and their derivatives of the template 3'-CC AGTAGT (ACACAT AGTAGT)$_2$ CC with 5'-TGTGTrA / 5'-TCATCrA (blue) or 5'-T^{bn}GTGTrA / 5'-T^{bn}CATCrA (orange) at pH 7.5 3mM CN^-.

Table S2, entry 3 :

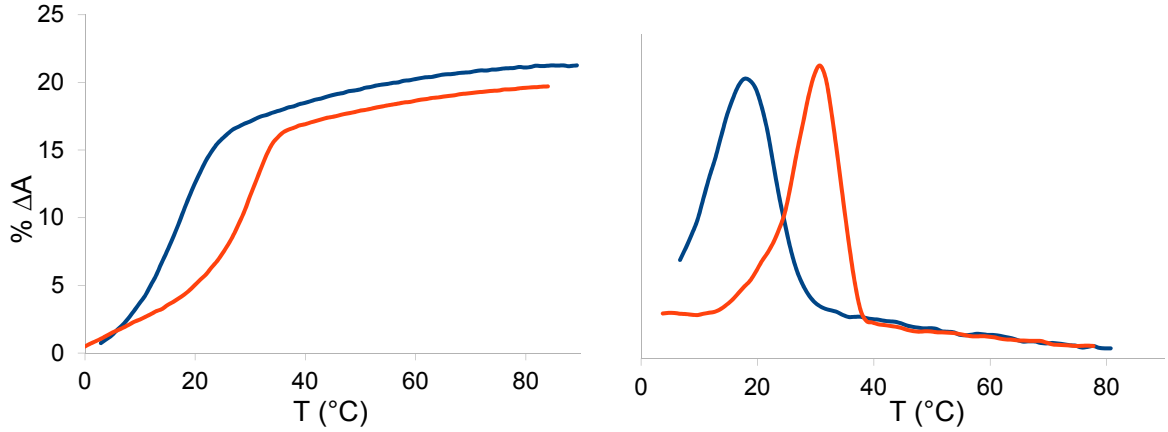

Melting curves and their derivatives of the template 3'-CC AGTAGT ACACAT AAAAAAA CC with 5'-TGTGTrA / 5'-TCATCrA / 5'-T$_7$ (blue) or 5'-T^{bn}GTGTrA / 5'-T^{bn}CATCrA / 5'-T^{bn}T$_6$ (orange) at pH 7.5 3mM CN^-.

Influence of mismatches on the assembly.

Table S3. UV thermal denaturation data with templates T_α mismatched on position 3.

Entry	Template	Template sequence[b]	Hexameric sequence[b]	T_m [°C][a] pH 7.5	T_m [°C][a] pH 9.5
1	T_α	3'-CC $(ACACAT)_2$ A*GTAG*T $(ACACAT)_2$ CC	5'-TGT**G**T**A**	26.3	24.3
			5'-T^{bn}GTGT**A**	28.3	34.3[c]
2	$T_{\alpha'}$	3'-CC $(ACACAT)_2$ AC*CT*AT $(ACACAT)_2$ CC	5'-TGT**G**T**A**	24.7	23.7
			5'-T^{bn}GTGT**A**	29.8	33.8[c]
3	$T_{\alpha''}$	3'-CC $(ACACAT)_2$ AC*C*CAT $(ACACAT)_2$ CC	5'-TGT**G**T**A**	23.8	22.8
			5'-T^{bn}GTGT**A**	30.8	35.2
4	$T_{\alpha'''}$	3'-CC $(ACACAT)_2$ ACACA*A* $(ACACAT)_2$ CC	5'-TGT**G**T**A**	24.8	24.9
			5'-T^{bn}GTGT**A**	33.4	36.4

[a]Melting temperatures are obtained from the maxima of the first derivatives of the melting curve (A260 vs temperature) recorded in a buffer containing 1 M NaCl and 10 mM of sodium cacodylate, Template concentration 3 µM, hexameric sequences concentration 15µM. [b]Mismatches are indicated in italic in template sequences; T^{bn} refers to boronothymidine and bold letters represent RNA residues. [c]High stabilization suggesting the formation of a stabilized bulge (See Figure S1).

Figure S1. Plausible bulge formation at pH 9.5.

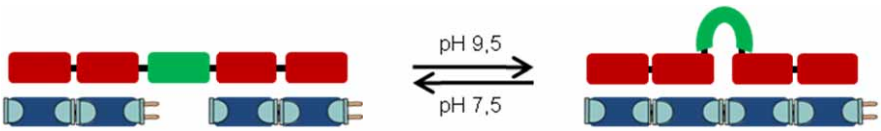

With T_α and $T_{\alpha'}$, high levels of stabilization are displayed at pH 9.5 suggesting the formation of a stabilized bulge between the 5'-end of section 2 and the 3'-end of section 4.

Table S3, entry 1 :

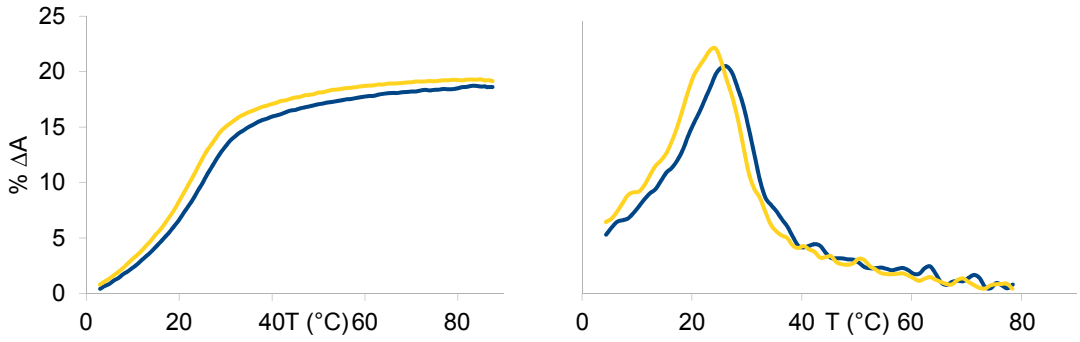

Melting curves and their derivatives of the complex 3'-CC-$(ACACAT)_2$-AGTAGT-$(ACACAT)_2$-CC / 5'-TGTGTrA 5 equiv at pH 7.5 (blue) and pH 9.5 (yellow).

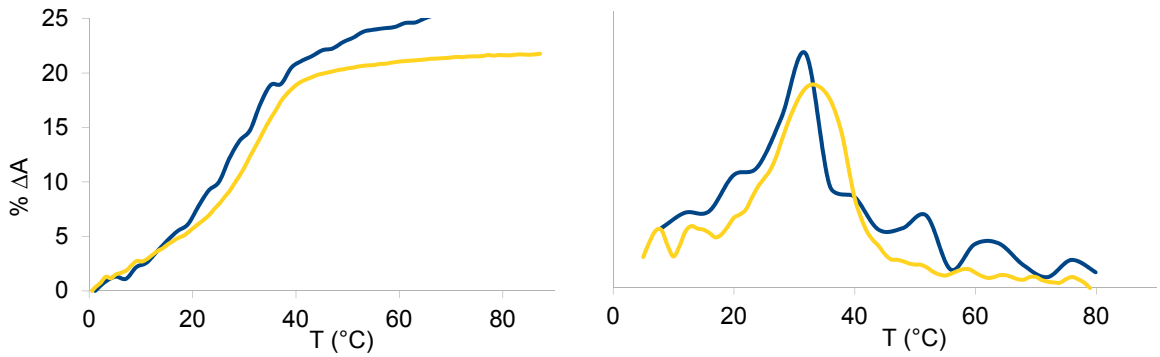

Melting curves and their derivatives of the complex 3'-CC-$(ACACAT)_2$-AGTAGT-$(ACACAT)_2$.CC /5'-T^{bn}GTGTrA 5 equiv at pH 7.5 (blue) and pH 9.5 (yellow).

Table S3, entry 2 :

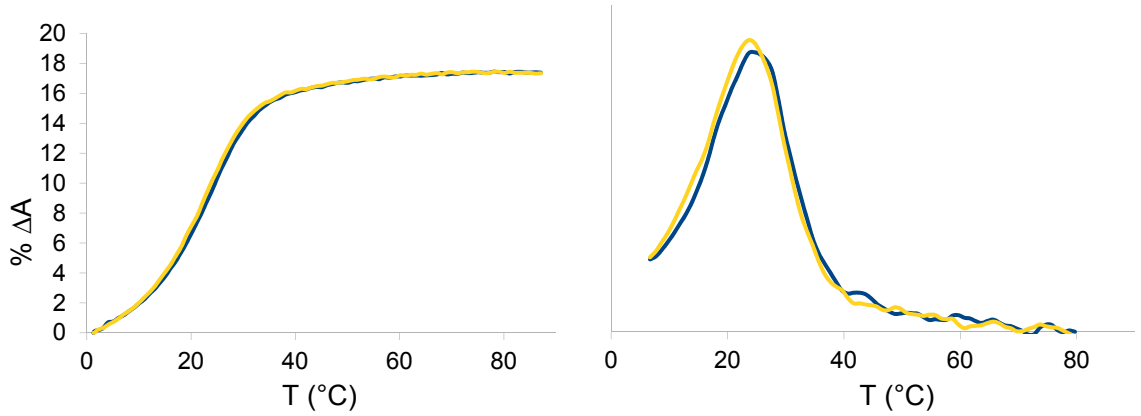

Melting curves and their derivatives of the complex 3'-CC-$(ACACAT)_2$-ACCTAT-$(ACACAT)_2$.CC / 5'-TGTGTrA 5 equiv at pH 7.5 (blue) and pH 9.5 (yellow).

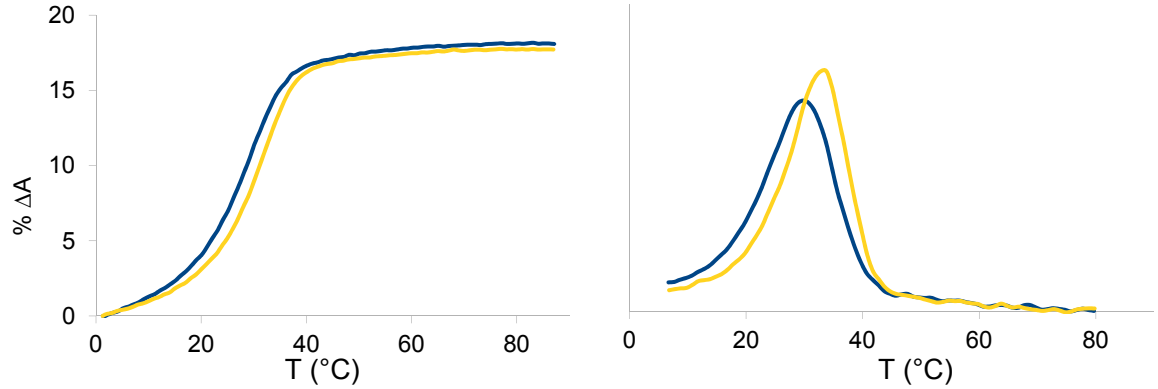

Melting curves and their derivatives of the complex 3'-CC-$(ACACAT)_2$-ACCTAT-$(ACACAT)_2$.CC /5'-T^{bn}GTGTrA 5 equiv at pH 7.5 (blue) and pH 9.5 (yellow).

Table S3, entry 3 :

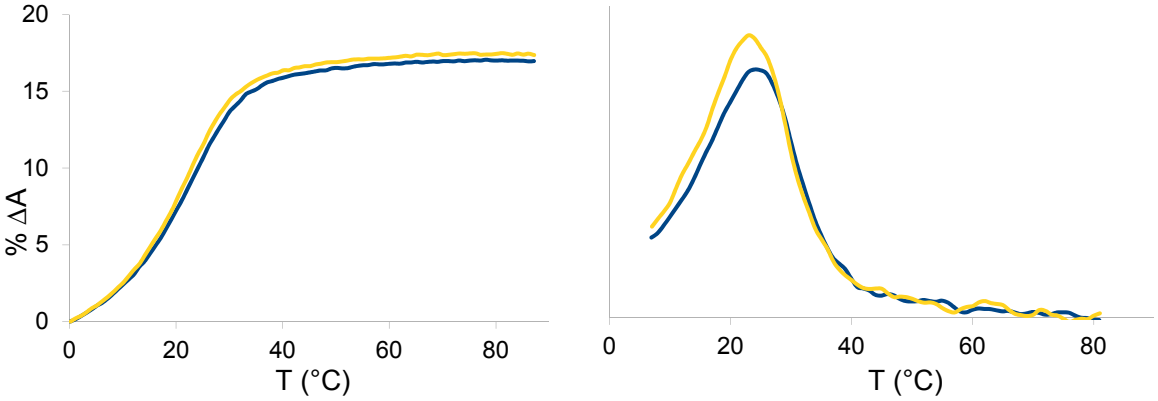

Melting curves and their derivatives of the complex 3'-CC-$(ACACAT)_2$-ACCCAT-$(ACACAT)_2$-CC / 5'-TGTGTrA 5 equiv at pH 7.5 (blue) and pH 9.5 (yellow).

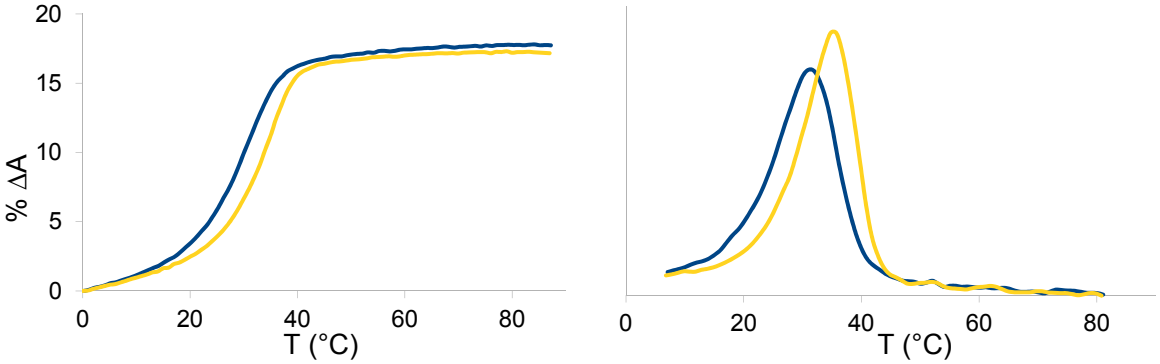

Melting curves and their derivatives of the complex 3'-CC-$(ACACAT)_2$-ACCCAT-$(ACACAT)_2$-CC /5'-T^{bn}GTGTrA 5 equiv at pH 7.5 (blue) and pH 9.5 (yellow)

Table S3, entry 4 :

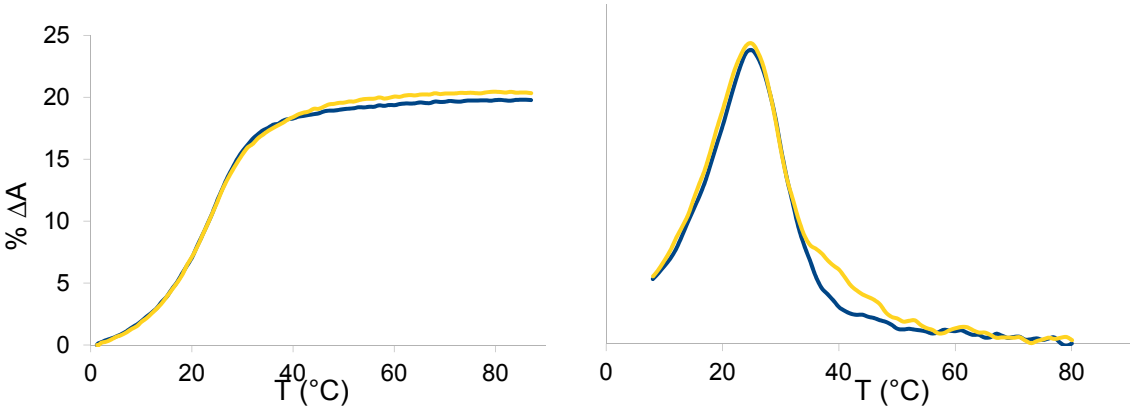

Melting curves and their derivatives of the complex 3'-CC-$(ACACAT)_2$-ACACAA-$(ACACAT)_2$-CC / 5'-TGTGTrA 5 equiv at pH 7.5 (blue) and pH 9.5 (yellow).

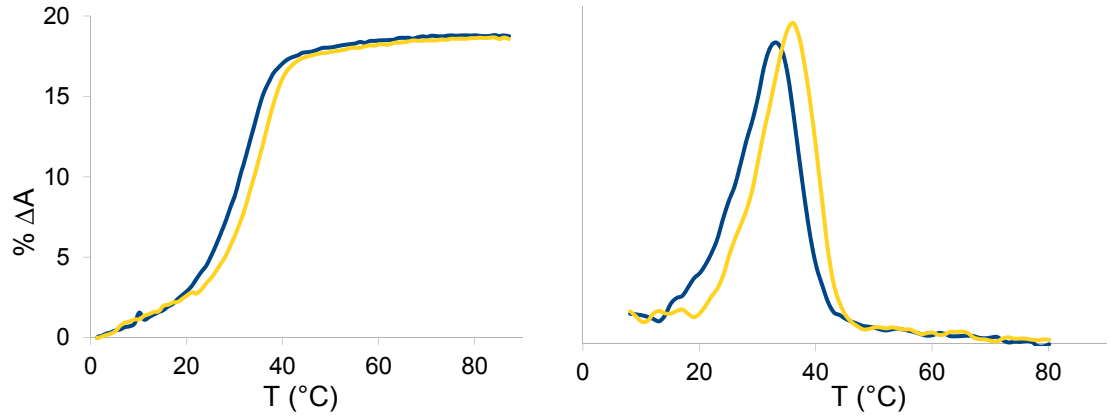

Melting curves and their derivatives of the complex 3'-CC-$(ACACAT)_2$-ACACAA-$(ACACAT)_2$-CC /5'-T^{bn}GTGTrA 5 equiv at pH 7.5 (blue) and pH 9.5 (yellow).

Native Polyacrylamide Gel Electrophoresis

Native PAGE experiments were performed with polyacrylamide gels prepared by mixing: TrisBorateEDTA (TBE) 1X solution, ammonium peroxodisulfate (APS), Acrylamide/N,N'-methylenebisacrylamide (19/1 v/v), and N,N,N',N'-tetramethyl-ethylenediamine (TEMED) in proportion shown below (Table S3). Freshly casted gels were pre-runned at constant power of 10 W for 40 min. After loading of the samples, run were performed at constant power of 10 W for the indicated time then revealed by UV shadowing.

Table S4. Reagent volumes for a 40 mL gel

Reagent	**Quantity**
APS	400 mg
TEMED	30 µL
TBE buffer (1X)	QSP 40 mL

Volume of Acrylamide/N,N'-methylenebisacrylamide	
For a 20% gel	20 mL
For a 15% gel	15 mL

Conditions of migrations :
Figure 2a : 20% native polyacrylamide gel, 120 min, 15 °C.
Figure 2b : 15% native polyacrylamide gel, 120 min, 15 °C.
Figure 2c : 20% native polyacrylamide gel, 100 min, 15 °C.
Figure 3d : 20% native polyacrylamide gel, 120 min, 15 °C.

Figure S2. Native PAGE with 5'-CC (TACACA)$_n$ CC (T_n, n= 2-6) as templates and 5'-T^{bn}GTGTrA (B) or 5'-TGTGTrA (C) as hexameric units.

Conditions : 20% native polyacrylamide gel, 120 min, 20 °C.

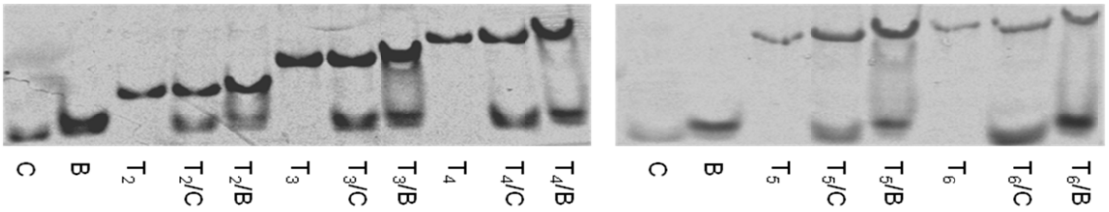

Neither boronic nor unmodified units hybridization was observed at 20 °C.

Figure S3. PAGE with mismatched T_α templates.

Conditions : 20% native polyacrylamide gel, 90 min, 10 °C.

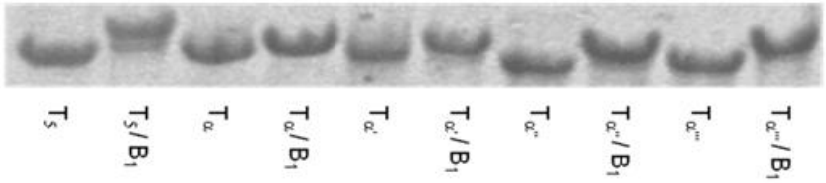

Mismatched T_α templates are compared to T_5 alone and in presence of B_1 5'-T^{bn}GTGTrA. Retarded bands are observed when only one mismatch is present either on central or terminal nucleotide of position 3.